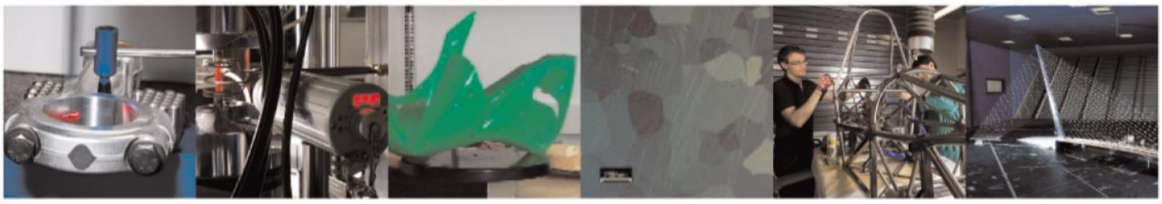

Challenges and Opportunities in the Selective Laser Melting of Biodegradable Metals for Load-Bearing Bone Scaffold Applications

Carluccio D.; Demir A.G.; Bermingham M.J.; Dargusch M.S.

This is a post-peer-review, pre-copyedit version of an article published in Metallurgical and Materials Transactions A. The final authenticated version is available online at:
https://doi.org/10.1007/s11661-020-05796-z

Challenges and opportunities in the selective laser melting of biodegradable metals for load-bearing bone scaffold applications

D. Carluccio[ac], A.G. Demir[b1], M.J. Bermingham[ac], M.S. Dargusch[ac]

[a] School of Mechanical and Mining Engineering and Queensland Centre for Advanced Materials Processing and Manufacturing (AMPAM), The University of Queensland, Queensland 4072, Australia

[b] Department of Mechanical Engineering, Politecnico di Milano, Via La Masa 1, 20156 Milan, Italy

[c] Australian Research Council Research Hub for Advanced Manufacturing of Medical Devices, St Lucia 4072, Australia

Abstract

The aim of this paper is to assess the current status of processing Biodegradable metals (BDM) via selective laser melting (SLM), with particular emphasis on bone scaffold applications, and provide a meta-analysis on the effect of processing parameters on relative density to better direct recommendations for the future of this growing field. Synthetic bone scaffolds are becoming a popular alternative for the treatment of critical bone defects that cannot heal without surgical intervention. These scaffolds act as a bridge allowing bone to grow across the gap. Selective laser melting can achieve bone scaffolds with complex hierarchical architecture tailored specifically to the patient. SLM manufactured titanium scaffolds have already been clinically tested with some success. Permanent titanium alloys have a higher chance of implant rejection from the innate immune reaction, coupled with complications linked to the high mismatch in stiffness between the implant and the bone. Biodegradable metals can overcome these problems by maintaining sufficient mechanical properties for load-bearing applications during healing and eventually

[1] Corresponding author: aligokhan.demir@polimi.it

degrade away completely. Currently, however, the use of SLM for the manufacturing of BDM scaffolds is still in its infancy as only a few peer reviewed studies are published, with the majority of these published in the last couple of years. Literature was systematically reviewed to critically analyze and synthesize the data in the form of a meta-analysis. Only studies that included the processing parameters used for volumetric energy density (namely the laser power, scan speed, hatch spacing, and energy density) and provided as built relative densities were used. SLM of biodegradable metals is an exciting research area that requires further exploration. Apart from overcoming the problems unique to each major biodegradable metal family, the meta-analysis showed that the vast majority of studies regard the optimization of SLM processing parameters. However, these studies are specific to the powder and machine used. Rather, broader guidelines need to be developed for modern SLM machines to allow for quicker optimization for future SLM manufactured BDM.

Keywords: Selective Laser Melting; Biodegradable Metals; Load-Bearing Bone Scaffolds

1.0 Introduction

Critical bone defects (CBD) are defined as bone gaps that will not heal without surgical intervention [1]. CBD anatomy can differ subject to the location, bone, and the patient. However, generally speaking, a non-osseous wound larger than 30 mm will not fully heal naturally [2]; instead, fibrous connective tissue forms [3]. Typically, CBD are not life threatening, but can greatly impact the quality of life of the patient [4]. The limitations incurred by treatment methods, such as autografts and allografts, sparked significant research into synthetic bone scaffolds [5-8], with some ceramic and polymer bone scaffolds already commercially available [9-11]. Yet, for load-bearing applications, these scaffold materials often do not have sufficient mechanical properties to maintain structural integrity during healing [12,13].

Permanent inert metals have been manufactured into bone scaffolds and tested *in vivo* with some success [14,15]. These scaffolds maintain their structural integrity throughout healing. In fact, the stiffness of these metals is often too high, and, along with their permanent nature, can lead to bone resorption and long-term complications [16-19]. Biodegradable metals (BDM) can overcome the problems associated with other bone scaffold materials for load-bearing applications; as they have adequate mechanical properties and, as the name suggests, are biodegradable, leaving no residue at the implant site following full healing. The three primary BDM families are magnesium, zinc, and iron-based alloys [20,21].

Investigation into the use of porous metals for bone scaffolds started in the late 20th century, after it was discovered that porous implants allowed for bone ingrowth [22]. Furthermore, introduction of porosity has been shown to reduce the stiffness of metals [23], reducing the stress shielding effect and subsequent bone resorption. By controlling the porosity levels and scaffold design, a balance between the mechanical properties, degradation rate, and bone ingrowth can be achieved. Traditional manufacturing methods for open-cell scaffolds, such as using space holder methods, powder metallurgy, salt-pattern molding, and direct foaming, allow for some control of the pore shape and size, but cannot achieve hierarchical porosity [22]. On the other hand, additive manufacturing (AM) techniques allow for control over the scaffold architecture [24,25]. Of these techniques, selective laser melting (SLM), can achieve the best dimensional accuracy allowing for highly complex scaffolds that can closely mimic the original bone structure.

Titanium bone scaffolds manufactured via SLM have already been clinically successful [26,27], showing the feasibility of SLM as a successful bone scaffold manufacturing method. The drawback of the permanent scaffolds can be overcome by using BDM. As mentioned above, BDM offer suitable mechanical properties for bone scaffold applications and can be manufactured using SLM. So far, Mg, Zn, and Fe alloys have been the only BDM successfully manufactured using SLM. The SLM of BDM for bone scaffolds is a very new topic, with only a handful of peer reviewed studies published, and the vast majority of these in the last few years [28]. This paper aims to survey the current landscape of SLM of BDM, and analyze current and future directions of biodegradable metal bone scaffolds manufactured via SLM.

2.0 Bone scaffold materials

Surgical intervention is usually necessary to treat CBD and allow for bone healing and remodeling. Autologous bone grafting has long been the “gold standard” treatment for CBD [29-31]. It involves harvesting healthy bone from a donor site in the patient, generally the iliac crest, and implanting it at the defect location. When compared to allografts and xenografts, autologous bone grafting is the most predictable treatment and has a lower chance of implant rejection reactions [32]. The high success rate though, does not mean autologous bone grafting is without its problems, for autologous bone grafting is synonymous with long term pain [33,34]. Since autologous bone grafting requires multiple surgeries, it has a higher risk of surgical complications and an elevated cost when compared to other methods used to treat CBD [32]. Donor site morbidity is the most common major complication from this procedure, often leading to chronic pain at the donor site [33,34]. Furthermore, in patients where the volume of the bone harvested from the donor site is less than that of the defect site (often occurs in pediatric and geriatric populations), autologous bone grafting is not a suitable option [32]. In this case, other bone grafting methods, such as allografts or xenografts, can be used.

Allografts are harvested from human donors and, as such, overcome issues associated with autologous bone grafting, such as donor site morbidity and donor site bone volume deficiencies. However, allografts can induce a significant host immune response and transmit infectious diseases from the donor to the host [35]. To reduce the host response allografts, the majority of allografts are typically demineralized or freeze-dried followed by irradiation, which also significantly reduces transmission of infectious agents and improve preservation of the graft. This comes at the cost of the mechanical properties and reduces the resorption and replacement rate during healing [35,36]. Furthermore, like other transplanting operations, a lack of donors has hindered the use of allografts. Xenografts have similar advantages and disadvantages to allografts [37], but since xenografts are harvested from animals, they are not limited by lack of donors. However, xenografts are even less predictable than allografts and, as such, have a higher chance of infection and rejection than autologous bone grafting [32].

Synthetic bone scaffolds fill the CBD providing a 3-D structure to allow for cell seeding, attachment, and subsequent proliferation leading to bone regeneration [38]. An ideal bone scaffold should:

- be fully biocompatible and ideally promote bone growth [39]
- have sufficient mechanical properties to match the host bone (Table 1) and allow for proper load transfer during healing [40]
- have interconnected pores with adequate pore size to allow for diffusion of oxygen and nutrients [40-42]
- be fully biodegradable leaving behind no residue in the implantation site [43]

Table 1 Mechanical Properties of Human Bone

Bone Type	Young's modulus (GPa) *	Compressive Strength (MPa)*
Cortical [44] [45]	1-35	90-205
Cancellous [45]	0.01-0.8	0.1-14

* The mechanical properties of bone can vary greatly depending on the age, type of bone and health of the bone.

For load-bearing scaffold applications, the scaffold should match the mechanical properties of cortical bone and maintain sufficient properties (i.e. at least a greater compressive strength than 90 MPa) throughout healing.

The first generation of metallic bone scaffolds primarily focused on biocompatibility and having sufficient mechanical properties [38,46]. Primarily made from metals such as CoCr alloys [47,48] and titanium alloys [14,15,49-57], these metals have had a long, successful history as inert and biocompatible orthopedic materials [38]. Biocompatibility is the ability of a material to accomplish its planned function without being toxic or eliciting undesirable immunological host response. However, this is often not a sufficient quality as these materials can promote the formation of fibrotic connective tissue at the tissue-scaffold interface that eventually surrounds the bone scaffold resulting in implant loosening. This is caused by foreign body granuloma, an innate immune response to foreign bodies that cannot be phagocytosed [38]. Furthermore, permanent metallic scaffolds have a higher chance of fragments breaking off over time, which may release toxic ions resulting in peri-implant cell death and bone atrophy [17-19]. Another limitation is that a large mismatch in mechanical properties between the implant and bone may result in stress shielding causing bone resorption [16,58,59].

To overcome foreign body granuloma, second generation bone scaffold materials were developed to be bioactive and stimulate positive biological host responses, such as osteoinduction [38,46]. Ceramic and polymer class materials have been developed to have excellent biocompatibility, encourage osteoblast adhesion, and promote bone growth [5,8,31]. These scaffolds have been successfully used in clinical trials, with commercially available ceramic and polymeric bone scaffolds having great success [9-11]. However, the mechanical properties of these porous bone scaffold materials are generally not suited for load-bearing applications, as the scaffold must maintain structural integrity during bone healing [60,61]. Another type of second generation material was designed to be biodegradable; ideally retaining its mechanical properties during healing and slowly degrading, transferring the stress to the newly formed bone without damaging it; subsequent to full healing, the implant would completely dissolve away without leaving behind any residue [38,46].

Biodegradable metals (BDM) can overcome the drawbacks of other second-generation bone scaffolds. BDM are defined as: "*Metals expected to corrode gradually in vivo, with an appropriate host response elicited by released corrosion products, which can pass through or be metabolized or assimilated by cells and/or tissue, and then dissolve completely upon fulfilling the mission to assist with tissue healing with no implant residues.*" [62]. For larger implants such as scaffolds, the bulk corrosion product should be an essential element the body can metabolize successfully in large doses [21]. Secondary corrosion products should be non-toxic and easy to metabolize. Essential metallic macronutrients include: Ca, Mg, Na, K, Fe, and Zn [63]; of these, Ca, Mg, K, Fe, and Zn are common dietary insufficiencies [64], and so implants made from these metals may in fact aid in supplementation of these insufficiencies. Of these metals, Ca, K, and Na are too reactive to be processed via selective laser melting (SLM). In fact, the majority of research on BDM has been based on Mg, Fe, and Zn as the major constituents [20,21,65,66].

2.1 Magnesium and alloys

Magnesium is an essential element [63] found mostly in human bones and the fourth most abundant metal found in the body (after Ca, K, and Na) [67]. It plays an important role in genome stabilization and is an important cofactor for many enzymes [68]. Consuming large doses of magnesium leading to Mg toxicity, which can result in muscle paralysis and cardiac and respiratory arrest, which rarely occur because it is processed and excreted in a very efficient manner [69,70]. For this reason, soon after the discovery of elemental Mg in 1808, physicians began exploring the surgical uses of pure Mg and its biodegradable properties with great interest [71]. However, it was not until the start of the 20th century that Mg was used for orthopedic applications, with limited success [71,72]. The high degradation rate of Mg may not be a problem with respect to its toxicity, but it is a problem for its mechanical integrity during bone fixation and subsequent bone healing [20,71,72]. The presence of impurities can further increase the corrosion rate as much as a thousand times [73,74]. Pure Mg also has poor ductility, which makes it difficult to manufacture into wires or screws [75,76]. For these reasons, it was mostly abandoned in clinical orthopedic practice in favor of more biologically inert and malleable metals as they became more readily available [77]. Despite these problems, research on Mg as a BDM for orthopedic applications continued due to its favorable properties. For example: it has a density close to that of bone [72], has been shown to promote osteogenesis [77,78] and has a modulus closer to that of bone when compared to Fe and Zn [72,79].

Significant research has sought to develop novel biodegradable Mg alloys containing low/non-toxic elements that can help improve both the mechanical properties and corrosion rate. In orthopedic applications, both are especially important as the implant will need to sustain the load to allow the bone to heal. If the implant degrades too quickly, the mechanical properties deteriorate too rapidly causing damage to the healing tissue. Furthermore, the fast degradation of Mg can lead to hydrogen evolution [73,77], which is especially dangerous in orthopedic settings, where blood flow is limited and, as such, mass transport is minimal. This can result in gas pockets causing tissue cavities [77,80,81] and damage to the healing bone [82]. Alloying elements must be biocompatible, and have a positive effect on the properties of the alloy. So far Mg-Ca based [73,74,83-91], Mg-Zn based [92-102], Mg-Si [102,103] based, Mg-Zr [102,104-107] based, and Mg-Rare-Earths [102,108-114] based alloys have been the most successful. However, substantial further research needs to be done in order to better control and understand the *in vivo* behavior of these new alloys [20,72,115,116].

Magnesium has a high strength-to-weight ratio and has been utilized extensively for weight reduction applications, and, because of this, numerous Mg alloys with good corrosion resistance and mechanical properties already exist on the market. The bio-corrosion of these commercial alloys has been extensively investigated [77,78,117-135]; however, they were designed for industrial use and many contain toxic elements such as Al or lanthanides [130,136-142]. The commercially available WE43 (containing Y, Rare-Earths, and Zr) is a high strength and corrosion resistant Mg alloy originally designed for aerospace applications. It has since become popular for biomedical applications due to its favorable mechanical and corrosion properties and low-toxicity corrosion products [77,143-145]. BIOTRONIK has successfully performed clinical trials on its modified WE43 stents marketed as absorbable metallic stents (AMS) [146-154]. MAGNEZIX® [155] is a European certified and commercially available WE43 based Mg alloy used for orthopedic screws [156,157]. Further clinical trials using high purity Mg were successfully performed in China, with patients showing higher healing results than the control group [158], leading to approval of high purity Mg screws as a medical device by the Chinese FDA. Similarly in Korea, RESOMET® (Mg-Zn-Ca) screws were approved after successful clinical trials showed normal healing results [159]. Porous Mg implants, however, are yet to be approved for clinical trials.

The ability of Mg to promote osteogenesis and thus promote implant integration and reduce healing time makes it an excellent candidate for bone scaffold applications [160]. However, the corrosion rate of porous scaffolds is greater than that of their solid counterpart due to the larger surface area exposed to the environment [161]. Furthermore, the Young's modulus of the scaffold is inversely proportional to its porosity level [162]. As such, additional challenges are faced by Mg for bone scaffold applications, since it is significantly affected by scaffold design [160,163,164]. Current research on novel manufacturing methods of topologically ordered scaffolds and coatings to reduce degradation rates and promote bone growth for Mg-based biodegradable bone scaffolds are promising [160,165-167].

2.2 Zinc and alloys

Zinc is an essential trace element [63] that is involved in critical physiological functions such cell proliferation and immunological and neurological pathways [168,169]. Furthermore, it regulates enzymes, proteins, and plays a critical role in DNA replication, stabilization, repair, and protection [168,170,171]. It is required in a dose of 8-11 mg/day, a dose less than 50 times that of Mg [172]. Daily intakes of zinc between 150-300 mg/day may result in zinc toxicity and doses higher than this can lead to serious health complications, such as neurotoxicity, reduced immune function and affect bone development [173].

Medicinally Zn has been used for thousands of years [174], however as a BDM, until recently, Zn had only been briefly investigated. In the 20th century, Zn implants led to discoloration around the tissue and research was promptly abandoned in favor of other metals [175]. Though within the last decade, significant research has been conducted on pure Zn and Zn-based alloys for biodegradable implant applications thanks to ground-breaking work by Bowen et al., who tested Zn wire in a simplified *in vivo* model and found it to have a favorable and controllable corrosion rate [176]. The same author then put forth a review paper making a case for Zn-based biodegradable stents [177], with the main drawback being its mechanical properties, as there remain concerns about the structural integrity during healing in load-bearing applications. Furthermore, the toxicity of Zn is debatable, and highly dependent on the implant setting [170,171].

Alloying Zn with biocompatible elements has been shown to improve the mechanical properties of Zn; Zn-Mg based [170,171,178-183], Zn-Ca based [171,180,184], Zn-Cu [185,186] based, Zn-Sr [180,184], Zn-Li based [187,188], Zn-Mn based [189,190], and Zn-Ag based [191,192] alloys have been successfully developed and tested. The majority of *in* vivo studies have been for Zn-based degradable stent implants [170,171,177], with only a handful of studies reported using Zn-based implants in orthopedic settings [193-195]. However, these studies used simple geometries, to date there have been no *in vivo* examinations into Zn-based orthopedic implants, such as screws or scaffolds.

Compared to biodegradable Zn-based stents, research on biodegradable Zn-based bone scaffolds has been relatively limited. Zhao et al. were the first to manufacture porous Zn scaffolds for bone applications and found that the mechanical properties were not sufficient for load-bearing applications [196]. Since 2018, over half a dozen papers been published on this topic [195-202], however, none of these studies reported Zn alloys that had sufficient strength for load-bearing (cortical bone) applications (Table 1) as porosity decreases the mechanical properties of the bulk material [203].

2.3 Iron and alloys

Iron is an essential trace element found mainly in hemoglobin and plays significant roles in human biology, including cell growth, transport and storage of oxygen, and reduction of RNA and DNA [204]. Being essential, it is required in a dose of 8-27 mg per day [172]. Iron can be toxic in high doses; however, iron toxicity is usually rare since iron levels are regulated through absorption [205]. Iron has a long history as an implant material with the first recorded iron dental implant dating back to 200 A.D [206]. In the 17th century, Fabricius used iron as a suture material for soft tissue defects and, over 100 years later, iron wire was used to set a broken humerus [207]. However, in these cases, Fe was used for its mechanical properties and manufacturability rather than for its biodegradable properties. It was not until the start of the 21st century that iron was explored as a possible biodegradable material [208].

Compared to Mg and Zn, Fe has excellent mechanical properties, similar to that of 316L stainless steel, a “gold class” metallic biomaterial [65,209]. However, the *in vivo* degradation rate of Fe is too slow and can thus invoke reactions similar to that of permanent metallic implants [208,210,211]. Furthermore, pure Fe is ferromagnetic which can impede imaging with magnetic resonance imaging (MRI) [65]. Significant research has been done on alloying Fe to increase the corrosion rate and improve MRI compatibility. To investigate the suitability of alloying elements for biodegradable pure iron, Liu et al. alloyed pure Fe with alloying elements commonly used in the iron industry, including Mn, Co, Al, W, Sn, B, C, and S [212]. Co, W, C, and S were recommended as suitable alloying elements based on the mechanical properties, biocompatibility, and improved corrosion rate. Other alloying elements like Au and Ga have also been researched with similar success [213-216].

Additions of noble elements past their saturation point in pure Fe, such as Pt (soluble up to 2 atomic %), Pd (soluble up to 3 atomic %), Au (soluble up to 1.4 atomic %) and Ag (soluble up to 0.02 atomic %), form noble precipitates forming small cathodic sites for micro-galvanic corrosion [217]. Increasing additions of Ag up to 5 wt. % were found to increase the corrosion rate, as more precipitates formed allowing for more micro-galvanic corrosion sites [215,218]. Similar results were found for additions of Au [215]. Huang et al. found that additions of 5 wt. % Pt resulted in slightly higher corrosion rates and mechanical properties when compared to additions of 5 wt. % Pd, with both alloying elements having higher mechanical properties and corrosion rate than that of pure Fe [216].

Manganese is an essential trace element necessary for bone growth and as a co-factor in enzyme reactions [219]. When alloyed with iron, it has been found to increase the corrosion rate of the alloy [220]. Furthermore, Mn promotes austenitic phase growth, improving the MRI compatibility and formability [209,221]. For these reasons, Fe-Mn based systems have been the most researched biodegradable iron alloys [209,220-227]. Hermawan et al. alloyed iron with Mn content varying between 20-35 % and found that higher concentrations of Mn doubled the corrosion rate and resulted in mechanical properties similar to that of 316 L stainless steel [209,222-224]. Similarly, sintered Fe-35Mn showed an increased degradation rate compared to pure Fe [228]. Capek et al. found that the potentiodynamic polarization tests showed that hot-forged Fe-30Mn had a higher corrosion rate when compared to pure Fe. However, the corrosion rate calculated from the static immersion test was lower than that of pure Fe. This was credited to localized rise in pH, that reduced the corrosion of the alloy [229].

Ternary and quaternary Fe-Mn based alloys have also shown success. Additions of Si created a shape memory alloy with improved mechanical properties and corrosion rate [230]. Twinning-induced plasticity (TWIP) steels have a long been used in industry [231] and some have recently been shown to have good biocompatibility [232]. Additions of Pd to TWIP steels significantly increased the *in vitro* corrosion rate by forming a noble intermetallic with iron. Further ageing allows the precipitates to finely disperse [220,226,232]. The *in vitro* corrosion rate of Fe-10Mn-1Pd was up to 10 times that of iron [220]. The *in vivo* corrosion of the alloy, however, was only slightly faster than that of pure Fe [233]. The cathodic reaction of the alloy is mass transport controlled [226], and since it was tested in an orthopedic environment, there was restricted blood flow, reducing the oxygen transfer and limiting the corrosion. Additions of silver to TWIP steel introduced ε-martensite during deformation, which, along with the Ag, reduced the ductility, but improved the overall strength [234].

Similar to permanent metallic implants, there still exists a mismatch in the stiffness between Fe and bone resulting in stress shielding and subsequent bone resorption [235]. Increasing the porosity level of the bulk material has been shown to reduce the stiffness [203], thus reducing stress shielding at the tissue-scaffold interface. Furthermore, increasing the porosity level increases the amount of surface area for cells to attach and proliferate, at the cost of the mechanical properties of the implant. Porous Fe-based scaffolds have been shown to have higher corrosion rates, and Young's modulus more similar to that of cortical bone [217,235,236].

3.0 Additive manufacturing of biodegradable metal load-bearing scaffolds

Additive manufacturing (AM) is defined as: "process of joining materials to make parts from 3D model data, usually layer upon layer, as opposed to subtractive manufacturing and formative manufacturing methodologies" [237]. The advantage AM has is that it can manufacture porous metal biomaterials for load-bearing bone scaffold applications with controllable porosity and scaffold architecture [24,25] as opposed to stochastic open-cell structures typical of traditional manufacturing methods.

Biodegradable porous metal scaffolds have been successfully manufactured using AM technologies such as binder-jet (BJP) and metal extrusion. BJP is a multi-step AM process in which a print-head selectively deposits a liquid binding agent onto a layer of powder. A fresh layer of powder is deposited on top bonding the materials together, the base is lowered, and this is repeated until completion of the component. In metal extrusion printing, the powder is mixed with the binder to form a slurry that is selectively deposited by a head. For bone scaffold applications, post-processing is necessary to increase the component strength. The binding agent is removed through curing followed by de-powdering, sintering, infiltration, annealing, and finishing [238,239]. These post-processing steps can be time consuming, costly, and result in a coarse microstructure [240]. As such, the mechanical properties of BJP components are typically not as good as their cast counterparts [241]. Furthermore since the powder is not melted, rather it is sintered, there exist a high chance of increased, and even varying, porosity in the component [242-244]. The surface finish and complexity of the part is also limited due to the binder and subsequent sintering. Extrusion based AM techniques also require binder, and, as such, have similar properties and require similar post processing to BJP scaffolds.

Porous Fe-30Mn scaffolds fabricated through BJP successfully increased the corrosion rate over ten-fold compared to bulk pure Fe [242]. However, the mechanical properties of the scaffold were not suitable for load-bearing applications. This was attributed to the formation of unexpected porosity due to poor packing of powder from irregular powder morphology. Hong et al. followed up on this work and manufactured Fe-35Mn-1Ca scaffolds using BJP [243]. They found that the corrosion rate was over double that of BJP Fe-35Mn and much higher than that of pure Fe. The addition of Ca reduced the ductility when compared to Fe-35Mn, and was significantly lower than that of iron; this was attributed to the limited resolution of BJP and unexpected porosity, likely due to irregular powder morphologies [243]. Mg-based metal extrusion resulted in a high-porosity composite scaffold with excellent biocompatibility, improved osteoblast differentiation, proliferation, and reduced bacterial adhesion [165,166]. The mechanical properties were sufficient for trabecular bone growth, but not for load-bearing situations. Similarly, Fe-based composite scaffolds manufactured through metal extrusion also showed improved osteoblast differentiation, with sufficient mechanical properties for low-load-bearing application [245].

Selective laser melting (SLM) is a laser-based AM technology wherein a laser selectively melts the component cross-section onto the powder bed. A fresh layer of powder is deposited on top and the process is repeated until completion of the part. SLM has become an increasingly popular method to manufacture bone scaffolds as it has better dimensional accuracy than other metal-based AM technologies and can thus achieve complex geometries with controlled pore size, distribution, and interconnectivity [14,54-57], without sacrificing mechanical and corrosion properties of the bulk material [246-248].

3.1 Selective laser melting of Magnesium and alloys

Porous Mg structures for bone scaffolds have been successfully manufactured using powder metallurgy (PM) [163,164,249-251], negative salt patterning [130,133,252,253], and laser perforation [254]. While Mg has been successfully manufactured via SLM, there remain concerns about processing the highly volatile

Mg powder. Furthermore, its high affinity for oxygen means oxide layers are formed easily, which can cause problems such as balling [255]. As such, the majority of initial studies were conducted on studying the ability to process Mg via SLM (processability) and attempting to achieve high density components (densification studies). Subsequently attention was turned to the characterization of SLM manufactured Mg parts to determine their suitability for biodegradable implants.

Ng et al. were the first to investigate SLM as a manufacturing method for Mg by melting single tracks of pure Mg powder using an in-house SLM machine [256]. Their future work identified the processing parameters (laser power and scan speed) required to manufacture Mg with similar mechanical properties to their cast counterpart [257-259]. The tracks did have a relatively large amount of porosity and defects as shown in Figure 1.

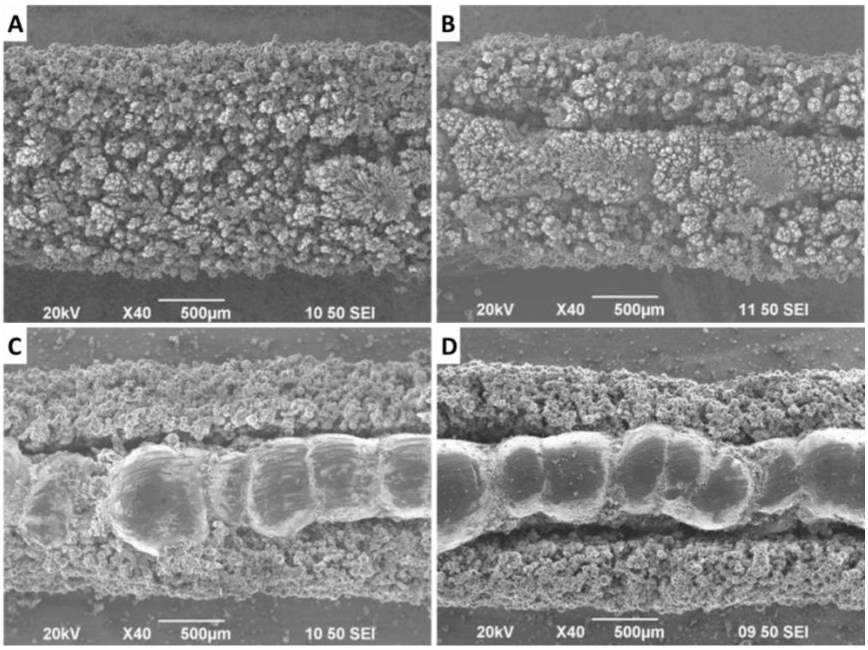

Figure 1 SEM images of surface morphology of pure Mg processed with a linear energy density of A) 0.33 J/mm^2, B) 0.66 J/mm^2, C) 0.99 J/mm^2, D) 1.33 J/mm^2. Reproduced with permission from [257].

This problem was also encountered by Zhang et al. during the SLM of Mg-9%Al [260]. During SLM of metals it is generally understood that an increased energy density results in higher density components, until a certain threshold is reached above which melt pool instabilities dominate and decrease the overall density of the part. The problem with Mg is that this processing window is much smaller due to the relatively small difference between the melting point of pure Mg (650 °C) and boiling point (1090 °C) [261], This presents a challenge to fully melt the powder without vaporizing it, which should be prevented because the recoil pressure from the vaporized material causes large pores within the solidified component. Zhang et al. managed to achieve a relative density of 82 % by varying the energy density and minimizing vaporization. Higher scan speeds result in lower energy density, which causes incomplete melting and encourages balling [260].

Wei et al. [262] and Schmid et al. [263] investigated the effect of energy density by varying hatch spacing and scan speed on AZ91D and AZ91 respectively. They found similar results to Zhang et al.; increasing the energy density initially increases the relative density and mechanical properties, but after an upper limit, any increase in energy density decreases the relative density and subsequently, the mechanical properties. SLM of AZ91D proved to be comparatively successful as the samples had a relative density of 99.52 % and showed a higher UTS, but a lower ductility, when compared to die-cast AZ91D [262]. Wei also investigated the effect of laser parameters on ZK60 and found that the maximum relative porosity achieved was lower compared to the AZ91D [264]. A follow up study by the same group found that increasing the amount of Zn content in a Mg-xZn alloy increases the amount of solidification cracking and decreases melt pool stability, resulting in increased microspores. Together, these defects significantly lower the mechanical properties of the alloy [265]. Like Mg, Zn has a relatively small difference between its melting point (420 °C) and boiling point (907 °C) [261]; therefore, a larger quantity of alloy was evaporated during SLM.

A research group at Fraunhofer led by Gieseke tried to overcome this by processing the Mg in overpressure in a modified SLM Solutions 125_{HL} machine. While this successfully increased its boiling point [266], the research was abandoned due to process instabilities in favor of a novel shielding gas circulation method [267]. The reactivity of magnesium powders poses a safety concern, which was amplified by the introduction of an overpressure in the SLM machine. The gas circulation method was introduced to remove the magnesium vapor, which can interact with the laser and cause processing instabilities, further amplifying the instabilities inherent of the highly volatile magnesium powder. Another factor in the improvement of relative density of SLM manufactured Mg components over time was the advancement in laser technology, and better understanding of powder particle interaction with the laser. This allows for better control of the actual heat input into the powder bed, resulting in less evaporation, and subsequent gas recoil instabilities.

Hu et al. were the first to manufacture bulk pure Mg using SLM by optimizing laser parameters and particle size, achieving a relative density of 95% [268]. It was found that smaller particles require a lower energy density to fully melt, but also produced rougher, less dense components with a higher number of defects. This is because a decrease in powder particle size, increases the friction in the bulk powder, promoting the balling effect. Smaller particles are also more sensitive to energy density, making it more difficult to control the vaporization of the Mg during SLM. Furthermore, since Mg needs to be selective laser melted in an inert environment, the smaller particles are more prone to be blown away by the cover gas [268]. Therefore, the larger particles produced denser and smoother components. The surface quality can also be improved by surface preheat, which also reduces warpage in single track manufacturing, but this effect reduces as layer thickness increases [269].

The first peer-reviewed study on the SLM of Mg specifically for biodegradable implant application optimized processing conditions using a bespoke SLM machine to manufacture high density pure Mg parts [270]. Using the same bespoke system, several studies into the effect of additions of various alloying elements on the microstructure, degradation rate, and mechanical properties of SLM manufactured Mg-based components were performed. In general, additions of alloying elements decreased the grain size with increasing alloying elements until a certain point due heterogeneous nucleation of grains on secondary particles, after which further additions increased the grain size [271-276]. The refined microstructure of the alloyed Mg improved its compressive strength, but further additions of alloying elements resulted in coarser grains and more secondary precipitations, reducing its mechanical properties. Conversely, the secondary particles increase the alloys hardness; therefore, the general trend was increasing hardness with increasing alloying content. The corrosion behavior followed a similar trend to the compressive strength and grain refinement, in that it decreased with increasing alloying content until it reached a peak, and subsequently increased with increasing alloy content [271-276]. This was attributed to two competing factors: the decrease in grain size, which reduced the corrosion rate, and the increase in secondary particles, which increased the corrosion rate. Decreasing the grain size generally increases the bulk uniform corrosion rate of the metal, as a higher number of grain boundaries increases the reactivity of a metal [277]. However, in simulated body fluids (SBF), decreasing the grain size stabilizes passive films, such as $Mg(OH)_2$ and MgO, that are formed during Mg degradation [20]. Increasing the number of secondary particles provides more sites for galvanic corrosion, which increases the overall corrosion rate; furthermore, as the number of secondary particles increase, the grain size also increases, therefore, further increasing the corrosion rate.

A recent study by Shuai et al. tried to decrease the corrosion rate of an Mg-3Zn alloy by using SLM to create a composite with hydroxyapatite (HA) [278]. When subjected to simulated physiological solution, HA is believed to react with the environment and form bonelike apatite on the implant surface [278,279] that slows down the corrosion rate. Similarly, increasing additions of β-tricalcium phosphate (TCP) to ZK60 manufactured via SLM decreased the corrosion rate up to a certain point due to the increasingly stable formation of HA during degradation [280]. However, too much addition of TCP reduced the relative density, exposing more of the composite to the environment, and thus, increasing the overall corrosion rate. Coatings can also be an effective method to reduce corrosion rate of SLM manufactured Mg-based biodegradable implants. Matena et al. coated porous Mg scaffolds manufactured via SLM with Polycaprolactone (PCL) to successfully decrease the corrosion rate and improve osteoblast adhesion [281].

To date only a handful of peer-reviewed studies have successfully manufactured porous Mg-based scaffolds via SLM as shown in Figure 2.

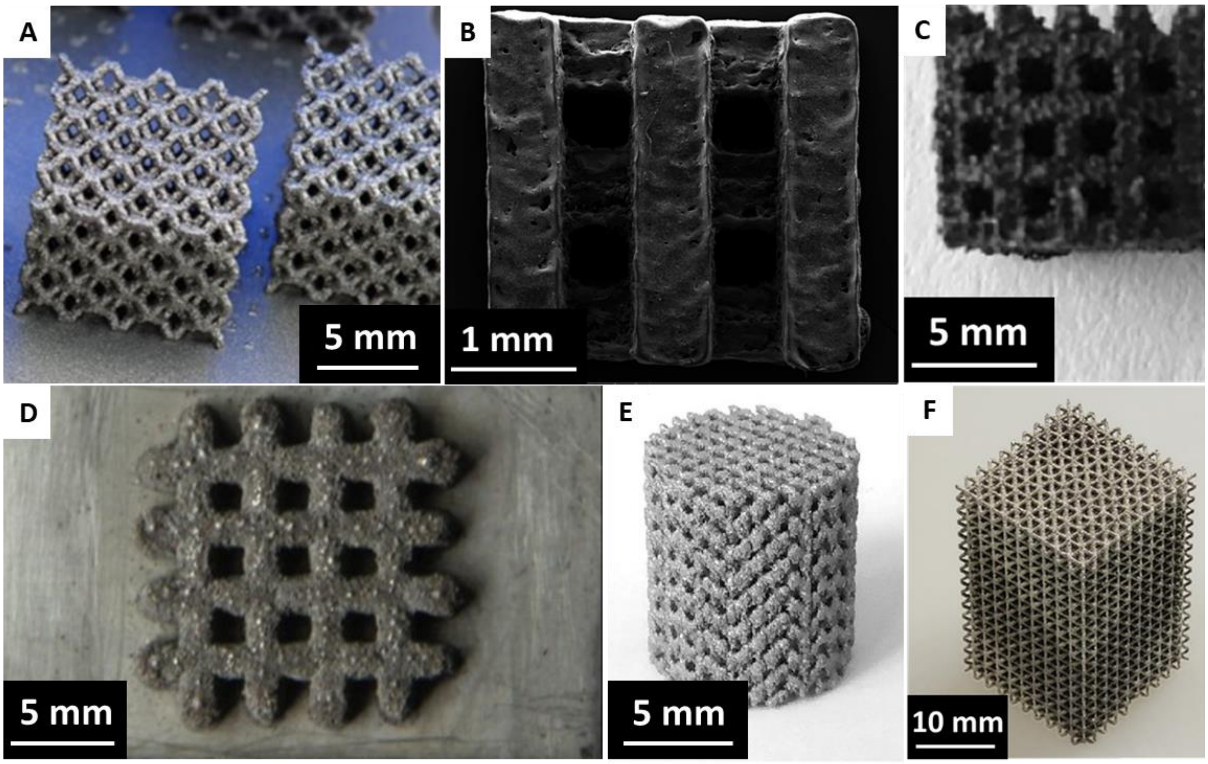

Figure 2 Magnesium based selective laser melted scaffolds. Reproduced with permission from A) [282], B) Reprinted from [281], under the terms of the Creative Commons CC BY license, C) [283], D) [270], E) [284], F) [285].

Jauer et al. were the first to successfully manufacture WE43 scaffolds with minimal strut porosity [286]. The authors employed a modified SLM system to overcome the issues created by vapor and fume formation during processing. The modified gas management system resulted in an improvement in part density through the removal of the fumes without perturbation of the powder bed. Using the same system, Witte et al. improved strut tolerances through process optimization and post-processing using sandblasting [287]. Other studies manufactured basic scaffolds while investigating the processing optimization of Mg [270] and Mg-Ca [283]. Similarly SLM manufactured Mg scaffolds were coated with PCL, with the focus of the study being on the coating [288]. The first full length peer-review study released was built on the works of Witte and Jauer et al. to manufacture and fully characterize WE43 diamond unit cell reticulated scaffolds manufactured via SLM for bone scaffold applications [284]. The study showed the feasibility of using Mg as a non-load bearing scaffold, as it maintained sufficient mechanical properties for trabecular bone even after 28 days of immersion in SBF along with adequate cytocompatibility [284]. Following up on this study, Li et al. investigated the fatigue behavior of SLM-manufactured WE43 [289]. It was found that degradation and fatigue were antagonistic; with increasing degradation, the fatigue strength decreased, and vice-versa with increasing fatigue, the degradation rate increased.

Kopp et al. were the first to investigate the influence of design and post-processing on SLM manufactured Mg-based scaffolds [285]. Reticulated scaffolds based of square unit cells were manufactured with varying pore size. These were then post-processed using plasma electrolytic oxidation (PEO), heat treatment, or both. Through PEO, the corrosion rate and hydrogen evolution are significantly reduced. Consequently, the degradation of mechanical properties over time is also reduced. However, both the PEO coated and non-coated samples had an increased corrosion rate and displayed more strut failure post heat treatment. This was attributed to segregation of the alloying elements at the grain boundary following the heat treatment, which promoted preferential corrosion at the grain boundaries [285].

It should be noted that in the studies above that mentioned the mechanical properties, the mechanical properties are not sufficient to match that of cortical bone, and as such, are not suitable for load-bearing applications. The architecture of the scaffold further invokes a higher corrosion rate as the introduction of pores increases the amount of metal exposed to the environment [161]. Since the mechanical properties are also correlated to the corrosion rate, a higher corrosion rate signifies a higher degradation rate of mechanical properties. Therefore, for load-bearing scaffold applications, not only do the mechanical properties need to be improved to match or better that of cortical bone, but it must also be ensured that the mechanical properties degrade at a sufficiently slow rate to allow for proper bone healing.

3.2 Selective laser melting of Zinc and alloys

As previously mentioned, the majority of research on Zn for biodegradable implant applications has occurred during the last decade. Compared to Fe and Mg alloys, the use of Zn based alloys in industrial applications is relatively limited due to its low mechanical properties. For this reason, there has previously not been a need to research the SLM of Zn. After the eminent study by Bowen et al. [177] the interest for processing Zn and its alloys by SLM piqued, with particular interest for biodegradable implant production. The recent interest means that the majority of studies to date have focused on processing Zn. The first peer-reviewed study on SLM of Zn was published in 2017 and found that, despite only obtaining a density of 88%, the mechanical properties were higher than their as-cast counterpart, likely due to the refined grains that are the result of the high cooling rates typical of SLM [290]. The high porosity level was attributed to the process instabilities of Zn during SLM; with low energy densities resulting in partial fusion of the powder, and conversely, high energy density leading to melt pool instabilities and, in the case of Zn, excessive evaporation. The difference between these two extremes for Zn is relatively small due to its small difference between the melting point (420 °C) and vaporization point (910 °C) [261] and therein, lies the difficulty in processing in Zn via SLM.

Zn vapor interacts with the laser and subsequently affects the processing of the powder bed. In closed chamber processing, this can compound as the vapor quantity increases [291]. When processed in a closed chamber, the Zn evaporated at a rapid rate, as shown in Figure 3, contaminating the chamber and reducing part quality.

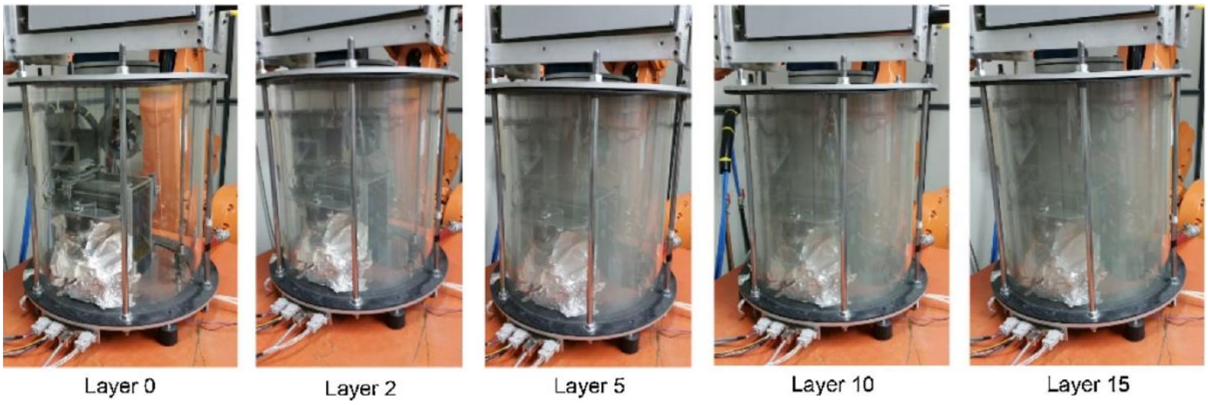

Figure 3 Contamination of SLM processing chamber due to Zn evaporation as layer number increases. Reproduced with permission from [291]

Since Zn is not as volatile as Mg, it can be processed safely in an open environment, with shielding gas flowing over the powder bed. In an open environment, the Zn vapor was removed and, subsequently, led to stable processing, achieving a density of over 99% and a hardness comparable to that of cold-rolled Zn [291]. The effect of particle size on density was similar to the results found for Mg [268] with coarse powder leading to higher densities.

Similarly, Wen et al. used an SLM machine equipped with a bespoke gas circulation system with slight overpressure to stabilize Zn processing and prevent the vapors from interfering. Using this system they optimized the processing conditions to achieve a high density (over 99.5%) part with mechanical properties higher than that of traditionally manufactured Zn [292]. This study was followed up by analysis of the surface quality of the as-build Zn component, which was comparable to other SLM manufactured metals. Furthermore, the samples were successfully sand blasted, resulting in a surface finish akin to other SLM manufactured metal components. The microstructure consisted of fine columnar grains along the build direction, with the average grain size much smaller than that of traditional manufacturing methods, leading to superior mechanical properties of the SLM manufactured Zn [293].

As mentioned previously, additions of alloying elements to Zn can successfully improve the bulk mechanical properties. For example, additions between 4-6 wt.%

Ag to Zn resulted in a significant reduction of the average grain size and transitioning the grain morphology from columnar to equiaxed. This was attributed to constitutional undercooling and the formation of the secondary Ag-Zn phase, allowing for heterogeneous nucleation. The reduction in grain size also resulted in better mechanical properties of the alloy. Furthermore, the fine dispersion of secondary particles acted as cathodic sites resulting in galvanic corrosion and increased degradation rates with increasing silver content [294]. Similarly, constitutional undercooling and heterogeneous nucleation on secondary phase precipitates resulted in decreased grain size with increasing additions of Mg. As a result, the mechanical properties were also improved. However, owing to a small potential difference between the bulk Zn and Mg-Zn precipitates, there was no accelerated degradation with increasing Mg content due to galvanic corrosion. Furthermore, increasing additions of Mg decreased the bulk degradation rate, and improved cytocompatibility [295]. The same group managed to optimize the SLM processing parameters to manufacture high density Zn-2Al components that displayed adequate cytocompatibility, tensile strength, and a good corrosion rate [296].

The use of SLM to manufacture Zn scaffolds is very novel, partly due to the previous low interest in Zn, and partly due to the difficulty in the SLM processing of Zn. Processing of bulk and fine (scaffold) geometries is inherently different [297]; therefore, it requires different processing parameter studies for the same material. Fine structures are more affected by processing instabilities and it can be very challenging to stabilize SLM of Zn. Successful examples of scaffolds produced by SLM are shown in Figure 4 [298-300].

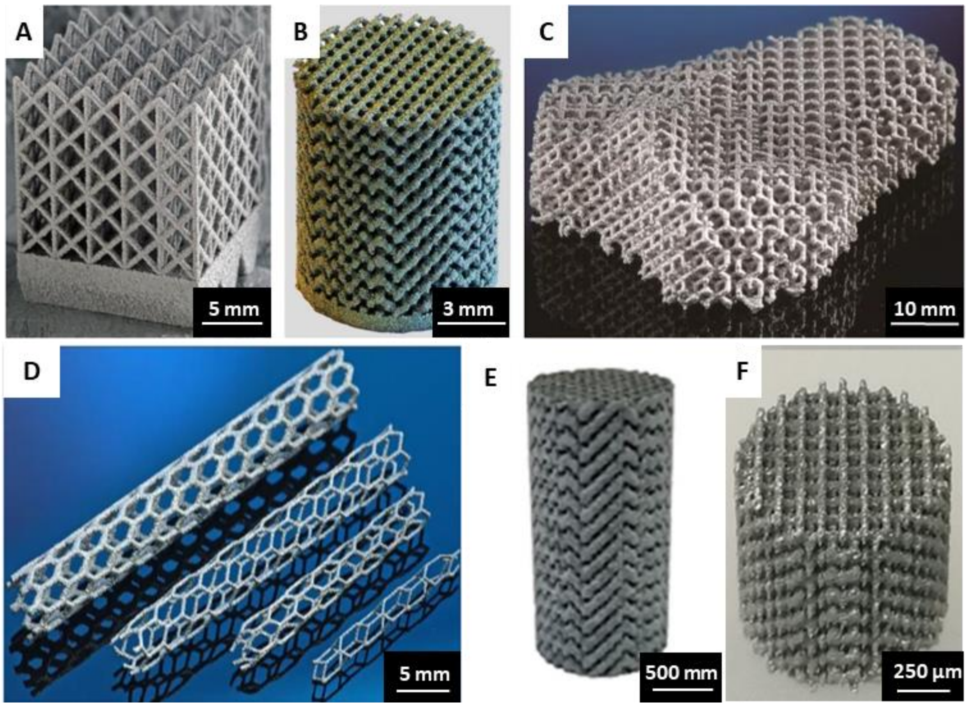

Figure 4 Zinc based selective laser melted scaffolds and stents. Reproduced with permission from A-C) [298], D) [293], E) [299], F) [300].

Wen et al. used SLM to manufacture both a Zn coronary stent and scaffold [293,298]. The former was a feasibility study, to show that SLM of Zn stents is possible; however, further testing is required. The latter was manufactured by using simulation to optimize the gas circulation and reduce the effect of the Zn vapor on the SLM process. Zn scaffolds were successfully manufactured with low processing porosity within the struts themselves. However, there was still substantial processing instabilities resulting in poor surface finish, which could be corrected by subsequent surface treatments leading to a suitable uniform surface finish, albeit with a strut size smaller than designed [298]. Mechanical and biological characterization of the SLM Zn scaffolds are currently on-going [66]. Qin et al. used the same gas-circulation method to investigate the effect of additions of WE43 to Zn on the formation quality, microstructure, and mechanical properties of SLM manufactured scaffolds [299]. High strut density was achieved for all samples, but there was significant partial sintering in the form of particles adhering to the struts, resulting in significant geometrical error between the designed scaffold and SLM manufactured scaffold. The mechanical properties increased with increasing WE43 up to 5 wt. % before reducing slightly. Overall additions of WE43 significantly increased the mechanical properties of the scaffold compared to pure Zn [299].

Li et al. were the first to characterize SLM manufactured Zn scaffolds [300]. They found that Zn scaffolds had suitable mechanical properties for cancellous bone, even after degradation. In fact, the mechanical properties increased after immersion testing, likely due to the formation of degradation product in the scaffold, rendering it a denser Zn/degradation product composite. Despite the formation of the degradation product, the degradation rate was still suitable for scaffold applications. Furthermore, the Zn scaffold displayed suitable cytocompatibility and cell viability. This study showed that SLM manufactured Zn scaffolds are promising for non-load bearing biodegradable scaffold applications [300].

3.3 Selective laser melting of Iron and alloys

Fe is an excellent bone scaffold material candidate, as its low corrosion rate and high mechanical properties allow for flexibility to optimize scaffold design [65,245,301,302]. Out of the 3 metals discussed in this review, Fe is the easiest to process via SLM; however, the majority of research on SLM of iron-based alloys has been on maraging steels, tools steels, and other steels used in industry [303]. SLM of iron and iron-based alloys for biomedical research has been very limited. Although not studied for biomedical purposes, several studies have achieved almost 100 % relative density of pure Fe by optimizing processing parameters to achieve ideal energy densities [304-307]. The majority of these papers focused on process optimization, and understanding the effects of SLM on the microstructure and mechanical properties.

Simchi et al. were the first to investigate the SLM of Fe but could not achieve a density above 75% due to insufficient energy input from the laser [308]. Over a decade later, high density Fe (shown in Figure 5) was successfully manufactured with mechanical properties superior to their traditionally manufactured counterparts [304].

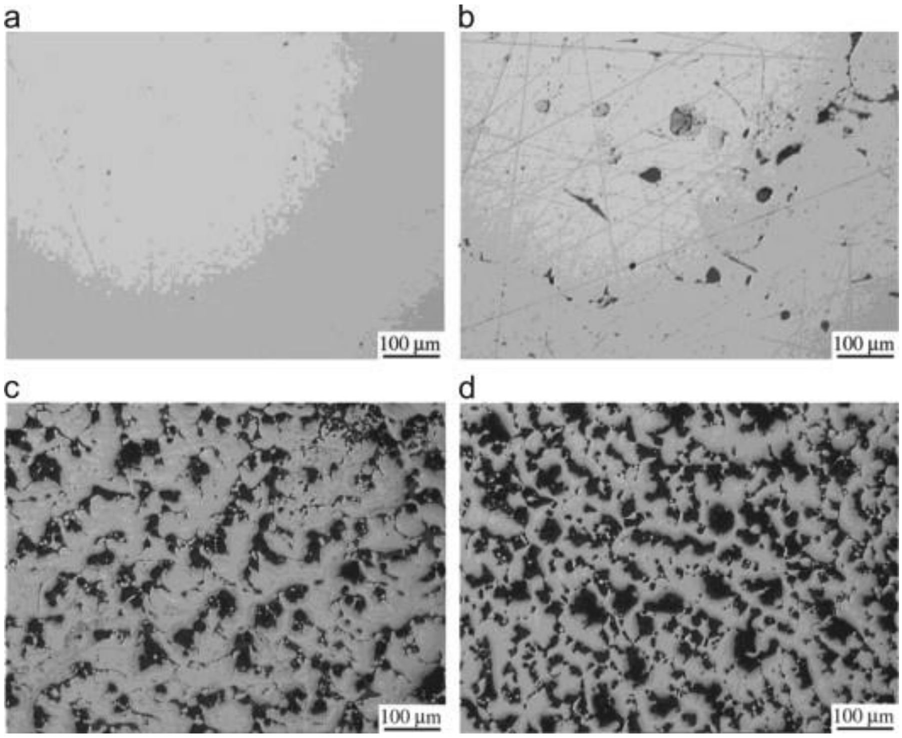

Figure 5 Cross sectional micrographs of pure Fe processed with a volumetric energy density of (a) 151.5 J/mm^3 resulting in a relative density of 99.3 %, (b) 100 J/mm^3 resulting in a relative density of 94.5 %, (c) 120 J/mm^3 resulting in a relative density of 82.5 %, (d) 90.9 J/mm^3 resulting in a relative density of 62.5 %. Reproduced with permission from [304].

Mechanical properties of the SLM Fe were further improved by vacuum annealing, which significantly reduced internal stresses [305] resulting from the complex thermal cycles and high cooling rates typical of SLM [309]. Similar to Mg and Zn, coarser powders resulted in higher density parts, which was attributed to an increase of laser transmissivity with increasing particle size [306]. However, if the powder size is too large, then a lower energy density will reach the lower part of the layer [306]. Other studies on SLM of pure Fe tried to reduce the cost of manufacturing by using cheaper water-atomized powder [307,310]. Despite the non-spherical powder having poor flowability and packing poorly, using SLM along with hot isostatic pressing (HIP), a density over 99.8% was achieved. To reduce cost and improve build rate the core of the sample was built at high speeds and the surfaces with low speeds to achieve a product with high density (after HIP) and suitable surface finish [310].

Investigations into using SLM as a process for manufacturing biodegradable Fe implants has garnered significant interest in recent years, with multiple studies coming out over the last several years. Montani et al. were the first to investigate the processing of pure Fe via SLM for biodegradable implant applications and achieved high density components, with the processability of pure Fe akin to that of 316L stainless steel [290]. 316L and Ti-6Al-4V are seen as the “gold standard” for biomedical metal implants, used for application ranging from aortic stents, to bone plates and screws. As such, having mechanical properties and SLM processability akin to that of 316L stainless steel, gives Fe based alloys a promising future to replace 316L for temporary implant applications such as stents, screws, plates, and scaffolds. In a direct comparison with other manufacturing methods, it was found that SLM pure Fe had a grain size significantly smaller than that of cast pure Fe, and as a result had superior mechanical properties [311]. Furthermore, the high density of internal defects and stresses imparted on SLM manufactured components increased the corrosion rate of pure Fe in simulated body fluid (SBF) [311].

Based on previous studies showing the positive effects of Mn additions on the degradation rate and mechanical properties of the alloy [220,223,226,227], high Mn twinning-induced plasticity (TWIP) steel powder was mixed with silver powder and processed via SLM [312,313]. By mixing the powders, Ag-particulates were distributed through the bulk TWIP steel, acting as local cathodic sites and increasing the overall corrosion rate [312,313]. As was the case with additions of Ag to Zn [294], increasing the Ag content increased the corrosion rate. The SLM processability of Fe-Mn alloys was actually found to be worse than that of pure Fe for solid components, but vice versa for scaffolds [314,315]. This was attributed to the larger melting range of the alloy, which, when using higher energy density typical of solid components, can result in more processing porosity. Despite this, using optimized parameters, high density components were achieved for both pure Fe and Fe-Mn parts[314].

As is the case with Mg and Zn, there exists relatively little literature on biodegradable Fe scaffolds manufactured via SLM.

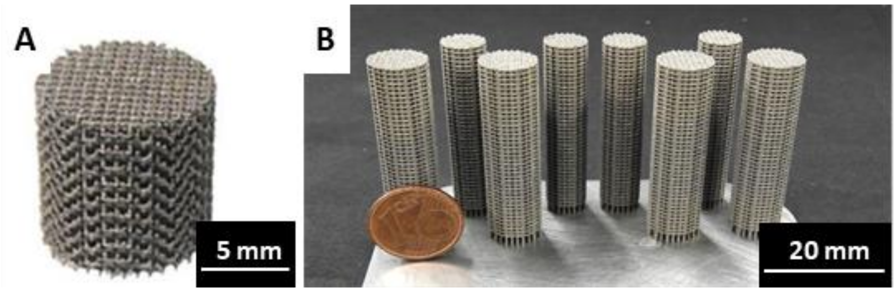

Figure 6 Iron based selective laser melted scaffolds. Reproduced with permission from A) [316], B) [317]

The first study to investigate this was in 2018, where Li et al. successfully manufactured a topologically ordered porous pure Fe scaffold via SLM [316]. This promising study found that the *in vitro* corrosion rate of the scaffold was much higher than its solid cast counterpart and, despite its accelerated corrosion rate it still showed acceptable cytocompatibility [316]. The accelerated corrosion rate is likely due to the synergistic combination of the manufacturing method and the scaffold design. The scaffold architecture increases the amount of metal exposed to the environment during immersion testing, which increases the corrosion rate. On top of this the complex heating and cooling cycles along with the high cooling rates typical of SLM imparts a high percentage of internal stresses, defects and dislocations. This combination can locally destabilize the passive film that typically forms on Fe when immersed in SBF [318]. Furthermore, unlike with Mg scaffolds [289], the pure Fe scaffold showed excellent fatigue strength minimally affected by degradation in SBF [319]. Following up on these studies, the same group investigated the effect of functionally graded porous pure Fe scaffolds on the permeability, mechanical, corrosion and biological properties [320]. It was found that through implementing functional grading the fluid permeability, and in turn biodegradation rate could be improved when compared to non-functionally graded structures. As such, this study presents the importance of scaffold design on the final properties of the scaffold.

Another study successfully manufactured both pure Fe and Fe-Mn scaffolds using SLM and found that the lower melting point of the alloy compared to the pure Fe was beneficial for the manufacturing of high quality scaffolds [315]. Following up on this study, Fe-Mn scaffolds were fully characterized, and it was found that the primarily FCC γ-austenite microstructure present lead to high ductility of the scaffold. This ductility and the mechanical properties were sufficient for load-bearing applications even after 4 weeks of immersion testing [317]. Similar to the Zn scaffolds [321], degradation product formed on the scaffold, which reduced the corrosion rate. Despite this, the combined effect of the scaffold design, manufacturing method, and addition of Mn led to much higher corrosion rates when compared to bulk pure Fe tested in a similar manner. The Fe-Mn scaffold showed good cytocompatibility; in fact, it showed excellent viability towards mammalian cells with filopodia attachment observed, signaling osteoblast adhesion. This was further shown by the first ever *in vivo* study on SLM manufactured biodegradable scaffolds which showed successful implant integration with the original bone, along with new bone formation after only 4 weeks of implantation [317].

3.4 Meta-analysis

The use of selective laser melting to manufacture biodegradable metal scaffolds is a very novel field, with the first peer-reviewed studies only being published in the last 5 years, as shown in Figure 7.

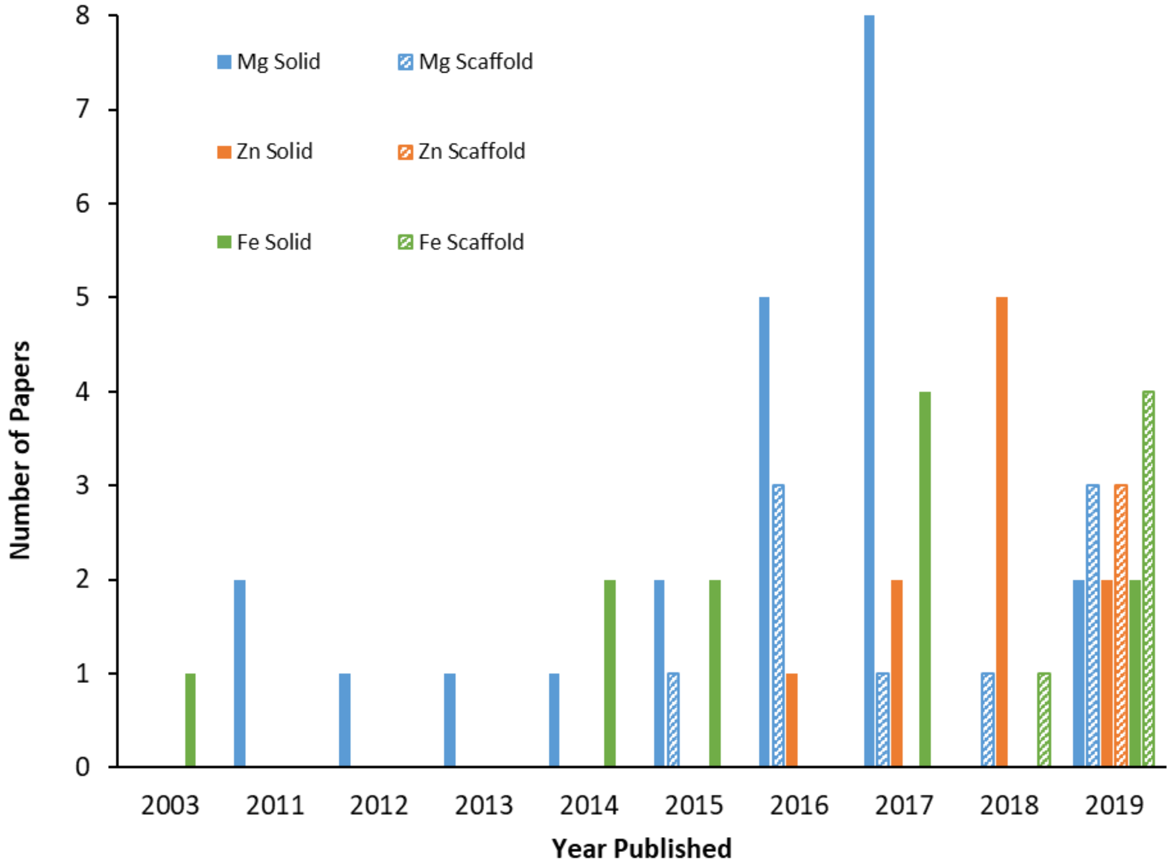

Figure 7 Number of peer-reviewed papers published per year on SLM of BDM

Mg-based alloys have been the most researched BDM; however, the majority of those papers were not specifically for BDM purposes. Indeed, Mg is a popular material for weight-reduction applications and it was not until 2016 that the first papers specifically for biodegradable implant application were published [270,271,273,322]. That year, the first studies on Mg-based scaffolds manufactured using SLM were published too [270,286,323].

Similarly, Fe-based alloys for industrial applications have been extensively studied [303] (not included in Figure 7), and as an extension, pure Fe has also garnered some attention. Yet, the first studies published on the SLM of Fe and biocompatible Fe-based alloys were not until 2017 [290,313]. With improvements in commercial SLM systems, more complicated reticulated Fe-based scaffolds could be manufactured, tailoring the otherwise unsuitable properties of bulk Fe to be suitable for load-bearing bone scaffold applications. After the ground-breaking study on SLM manufactured Fe scaffolds by Li et al. in 2018, the number of papers published in 2019 has increased 4-fold.

Unlike Mg and Fe, Zn is not commonly used in industry, so research on SLM of Zn was not an active research area until 2017, when the first SLM feasibility studies on Zn were published (around the same time that SLM of Mg and Fe for biomedical applications was investigated) [290,291]. Since bulk structures are easier to manufacture than scaffolds, all of the studies published in 2017 and 2018 focused on overcoming the SLM process instabilities of Zn, before subsequent studies focused on scaffolds in 2019. In fact, for all BDM, research on SLM to manufacture scaffolds is slowly overtaking that of bulk materials. The difficulties and cost in manufacturing BDM using SLM is only appropriate if the final component cannot be manufactured using traditional manufacturing methods, as is the case with fine structures and geometries, such as stents and complex scaffolds. Indeed, this is what the authors believe is the future direction for SLM of BDM.

3.4.1 Process parameters

SLM has a host of processing parameters that relate to the final part quality [324]. The general consensus in literature, however, is that laser energy input combined into one index (the energy density) is one of the best predictors for part quality [303,324]. It is important to note that this is generally true for bulk components[66] but not for scaffolds, where there does not appear to be any direct correlation between the usual quality indicators and the volumetric energy density [315].

Volumetric energy density (VED) is the preferred iteration of energy density for SLM [66], represents the amount of energy density per unit volume and is given by a combination of key processing parameters as shown in equation 1 [325]:

$$VED = \frac{P}{v \times h \times z} \qquad (1)$$

Where P is the laser power (W), v is the scan speed (mm/s), h is the hatch spacing (mm), and z is the layer thickness (mm). For lasers operating with pulsed wave (PW) emission by power modulation, the scan speed can be simplified as d_p/t, where d_p is the point distance referring to the distance between consecutive laser pulses and t is the pulse duration. The relationship between hatch spacing and spot size is also important for SLM processing, relating especially to the process stability [303,326]. This relationship helps explain the effect of laser beam overlap between scan lines on the relative density. Typically, this ratio is reduced to allow for higher productivity (by increasing the scan speed) while maintaining high relative densities.

A meta-analysis was performed to investigate the effects of volumetric energy density and linear energy on the relative density of SLM manufactured BDM bulk parts. Only peer-reviewed studies that provided in depth processing conditions were included in the meta-analysis. Studies that included post-processing to increase density, such as hot isostatic pressing (HIP), were excluded. From Figure 8 A,C,E, it can be observed that there exists no clear processing window for Mg as there is for Zn or Fe. In general, there are three distinct processability zones. When the energy density is too low, there is insufficient energy to fully melt the powder; instead, only partial sintering occurs, resulting in high porosity due to lack of fusion. On the other hand, if the energy density is too high, then melt pool instabilities and evaporation occur, reducing the relative density due to porosity related excessive energy or keyhole formation. In the middle, there exist the zone known as the processing window, wherein the energy density is suitable to achieve high density components.

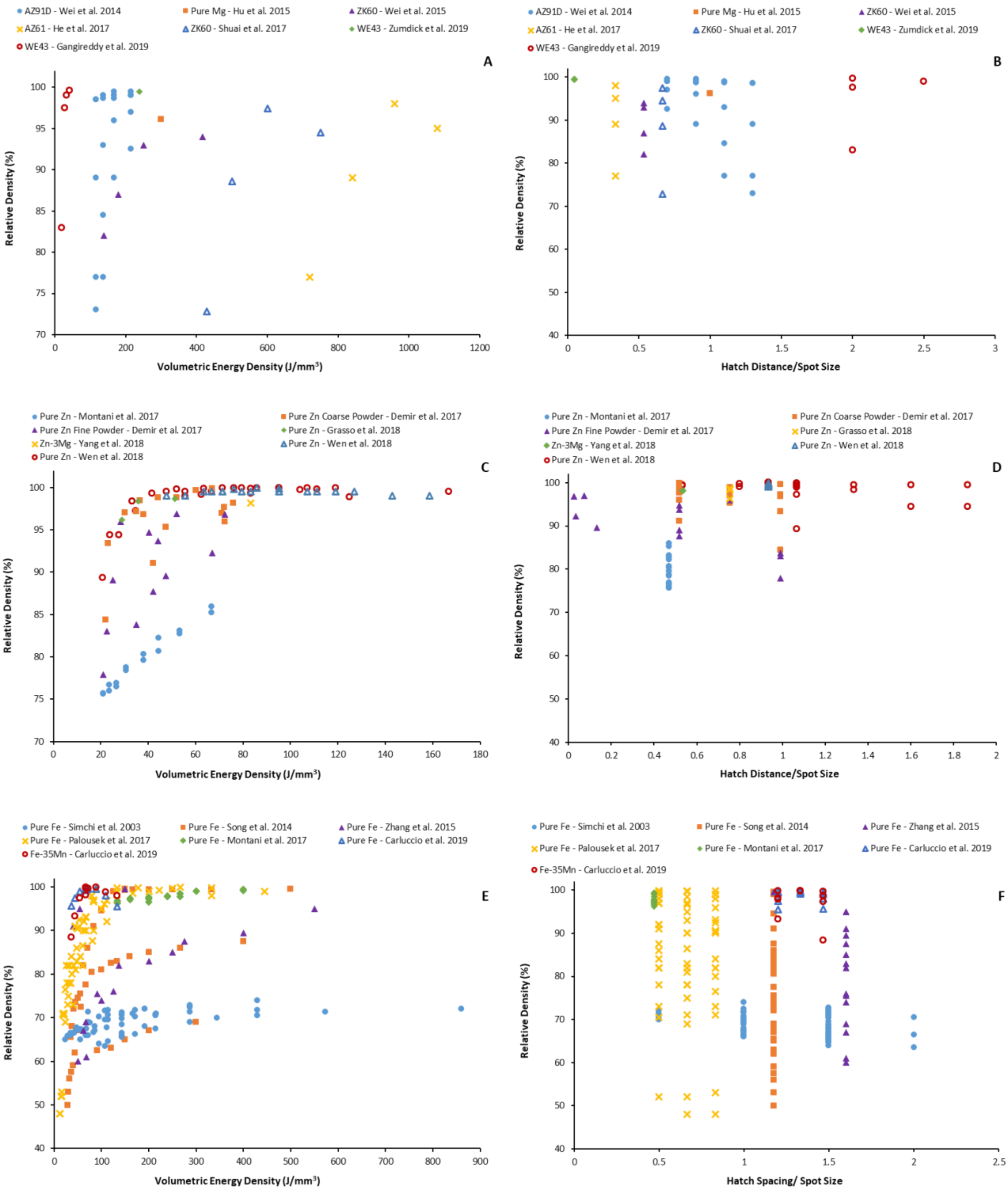

Figure 8 A) Effect of VED on relative density, B) Effect of hatch spacing to spot size ratio on the relative density, for Mg-based alloys; C) Effect of VED on relative density, D) Effect of hatch spacing to spot size ratio on the relative density, for Zn-based alloys; E) Effect of VED on relative density, F) Effect of hatch spacing to spot size ratio on the relative density, for Fe-based alloys [260,262,264,268,274,290-295,304-308,310,311,314,327-331].

For Zn there exists a processing window around a VED of 40-100 J/mm_3, in which multiple studies achieved high density components. The processing window can be seen even more clearly for Fe (Figure 8 E), where a VED of approximately 50-400 J/mm^3 leads to high relative density components. On the other hand, for Mg there exists no such processing window, rather, all of the studies shown achieve high density components using different VED, with no real agreement between them. The larger variation of results for the Mg alloys also reflects the progression in research efforts throughout the last few years. The excessive vapor generation leads to a highly instable process, while the low density limits the use of increased gas flow, which can disturb the powder bed. As such, initial efforts had limited success. By the introduction of in-house made systems and enhanced gas flow management systems, the processability of these alloys was improved. Observing a clear trend from the meta-analysis is difficult as the SLM system specifications dominate over the processability. This is further highlighted in Figure 8 B, wherein it can be observed that the hatch spacing to spot size ratio for high density components varies greatly, attributed mostly to researchers trying to stabilize the process (since hatch spacing/spot size greatly affects process stability) by investigating a wide range of parameters.

Such issues concerning excessive vapor generation during the SLM process exists also for Zn alloys, as such similar to Mg, the hatch spacing/spot size ratio is widely varied to improve process stability. However, compared to Mg, more success was found due to the higher material density, making the gas management relatively easier. It should also be noted that the interest on processing Zn by SLM has emerged more recently and has focused almost entirely towards biodegradable implants. Therefore, the issues concerning the process instabilities were quickly identified and tackled. Indeed, most of the papers available in literature employ in-house built or modified systems with novel gas management concepts. It is interesting to observe that the density improvements are almost correlated with the publication years showing the advancements in the SLM systems. However, it can still be observed that the processing window of Zn is much smaller, occurring in between a VED of 40-180 J/mm^3. This is attributed to the high instability of Zn during SLM process due to its low difference in melting and boiling points. The meta-analysis of Zn should be treated with caution however, as the main novelty in processing Zn lies in stabilizing the process through various techniques such as processing in an open atmosphere [290] or using a novel gas circulation system [292].

Fe-based alloys are relatively stable and have been shown to be easy to process [303]. Indeed, for Fe-based alloys, the processing window lies approximately between 40-500 J/mm^3, which is larger than that of Zn based alloys. The better processing stability is also shown by the smaller hatch spacing/spot size ratio in Figure 8 F. The use of SLM for processing Fe-based alloys for biodegradable implant applications has significantly increased in the last few years and, since it belongs to the oldest class of materials studied for SLM, higher relative densities are achieved as the publications are more recent. Concerning the Fe alloys, it should be noted that not only the SLM machine architecture but also the powder production methods and size distributions have been optimized throughout the years allowing for a more stable process.

The meta-analysis conducted highlights one of the key challenges that is faced with SLM of BDM scaffolds. The majority of studies discussed in this review are process optimization studies, but these only work on a specific powder for a specific machine. While these process optimization studies show the effects of various processing parameters on important qualities (such as relative density) of the final component, a holistic, all-encompassing approach, for modern SLM machines, should be developed. These guidelines will to allow for quicker optimization, allowing future studies to focus more on other aspects of BDM scaffolds that require further research.

3.4.2 SLM system for BDM

The challenges concerning the production of BDM implants by SLM differ compared to the permanent implant materials such as Ti-6Al-4V. The key issue is the low processability of these materials owing to their physical properties but also their intrinsic reactivity. The high reactivity of the material combined with increased reactivity of being in powder form renders the SLM process a safety concern as well. The oxidation enthalpies of pure Fe, pure Mg, and pure Zn are −260, −602, and −343 kJ/mol [332] respectively. As seen in Figure 9, bespoke SLM systems have been widely used for processing BDM, which reflects the complications related to the process. Researchers have used in-house made systems [271,290,291], as well as commercial lab-scale open systems [284,298,299] and modified commercial machines [315,319].

As most of the commercial SLM systems fail to address the processability issues related to BDM, some of the most critical factors regarding the SLM system configurations can be outlined. Arguably the most important factor is related to the gas management and filtration systems, since they play a key role in machine and operator safety as well as process stability. Moreover, Mg and Zn based powders tend to oxidize more quickly compared to the common SLM materials and may absorb more humidity from the ambient air. Therefore, the oxide and hydrogen release during the process can be problematic. Under these conditions, the laser diffusivity is decreased. Laser power is lost, while the beam profile reaching the powder bed is expected to be different. The process plume and vapor expand rapidly generating a pressure front, which can cause denudation in the processing zone. Most of the commercial SLM systems operate with a gas flow pushing the process plume, vapor, and debris away from the powder bed. However, for Mg and Zn, the gas flow should be assisted also with a suction system for a more effective evacuation. On top of this, as outlined above, the lower density of Mg powders means that the gas circulation system must be tailored to ensure the powder bed is not disturbed during processing.

Powder spreading and powder bed packing are other factors that are also more important for BDM compared to conventional SLM materials. The excessive vapor generation with Mg and Zn and oxygen release during the processing of Fe may cause severe denudation. Accordingly, more compact powder beds may be beneficial for the purpose. The use of different powder release mechanisms and recoating systems are yet to be analyzed from this perspective.

Concerning the laser sources, the most common choice, which is the active fiber laser, appears as an appropriate choice due to sufficient optical absorptivity for all material types (solid materials at room temperature A_{Zn}= 55%; A_{Fe}= 35%, A_{Mg} = 7%) [333-335]. On the other hand, temporal and spatial beam shaping features can also be used, which include the beam spatial profile, the emission mode, and scan strategies.

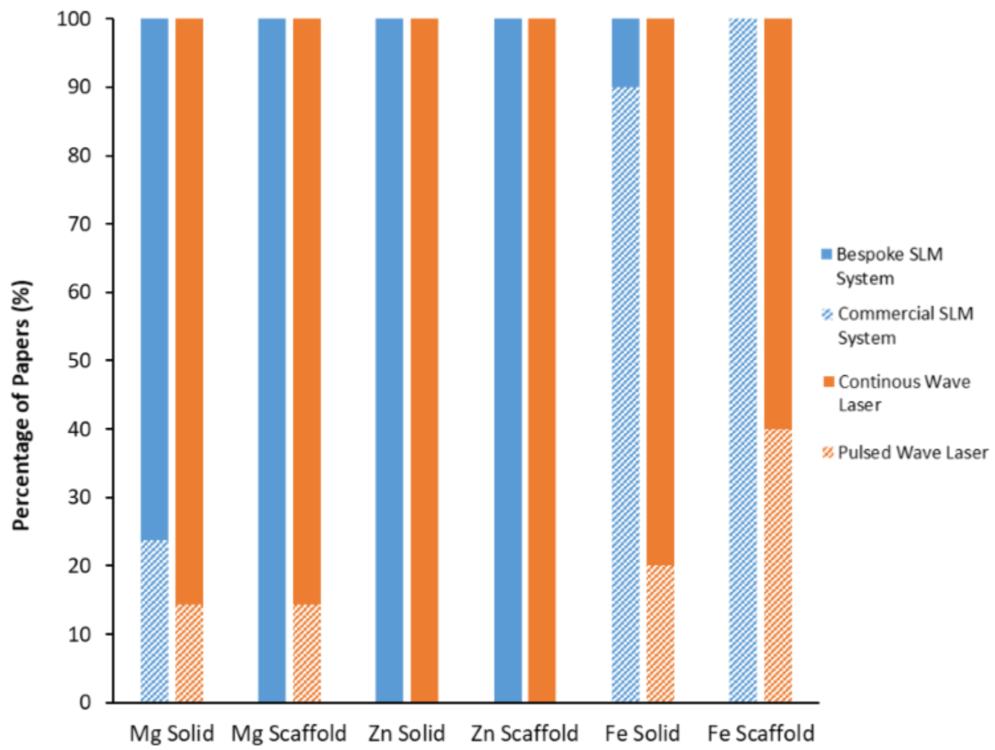

Figure 9 Percentage of peer reviewed papers using bespoke SLM systems Vs commercial SLM systems and using CW lasers Vs PW lasers for BDM.

The most common beam spatial profile used in SLM systems is the Gaussian profile. Researchers have shown that different profiles can be used to control the temperature profile as well as the cooling cycles [336-338], allowing for better control over the final components microstructure.

Regarding the emission mode, the conventional fiber lasers can operate both in continuous wave (CW) lasers and pulsed wave (PW) (by power modulation) lasers [339,340]. Several studies have shown that PW lasers allow for a more flexible control of the heat input through regulation of the individual laser pulse overlaps (pulse distance) and the laser impulse time [339-342]. As such, PW lasers are preferred for fine geometries, such as scaffolds, as they are sensitive to heat input. Furthermore, PW emissions allows for more accurate positioning of each laser pulse when compared to CW laser scan lines, allowing for better geometrical accuracy and integrity [339-342]. However, the inherent intermittent heat input of PW lasers can result in higher melt pool instabilities. Conversely, the continuous heat input associated with CW lasers increases the thermal load, resulting in better melt pool stability and wider melt pools [342,343]. Additionally, CW lasers have a higher melting efficiency and as a result a higher build rate when compared to PW lasers [342].

When selective laser melting solid parts, high relative density is one of the most important final attributes. As such, the majority of studies prefer CW lasers over PW lasers, as can be seen in Figure 9, since CW lasers can achieve higher density components [339-342]. Similarly, for highly unstable materials such as Mg and Zn, wherein melt pool stability is critical, CW lasers are preferred. On the other hand, for a stable material like Fe, PW systems would allow for more complex scaffold architectures when compared to CW. However, since majority of commercial SLM systems employ CW lasers, it is still the predominant laser emissions system for Fe based scaffolds [339].

Different scan strategies in SLM have been most widely studied for the cracking phenomenon [344,345]. Such strategies can be potentially used to better manage the vapor generation and denudation phenomena. On the other hand, most of the conventional scan strategies fail to address the difficulties regarding the fine details required for the thin struts with dimensions smaller than 1 mm. Contour scans [346], single line [347], and single point exposure [348] strategies have been proposed for conventional SLM materials, which are appropriate for BDM scaffolds.

Finally, the need for in-situ process monitoring techniques should be more effectively investigated for processing BDM with SLM both for internal defects as well as dimensional errors [349]. Beyond the formation of common defects such as lack-of-fusion or excessive energy pores, it has been reported that Zn exhibits component collapse due to material ejection indicated by an unstable plume behavior [350].

4.0 Design considerations for SLM manufactured load-bearing bone scaffolds

Scaffold geometry can significantly affect the mechanical properties, and also the degradation rate, cell ingrowth, and subsequent cell proliferation [351,352]. This has resulted in significant research on scaffold geometry optimization for bone scaffold applications [352-356]. It is well known that mechanical properties are inversely proportional to the level of porosity [203], with circular pores improving the stiffness of the scaffold when compared to cylindrical pores [25]. Topologically optimized scaffolds have fewer stress concentrations, lower maximum stresses, and relatively uniform Von Mises stress distribution resulting in better strength-to-weight ratios [356-358].

Porosity level and pore size of the scaffold can drastically affect both the cellular response and subsequent tissue regeneration during healing [25,351,352]. Open-cell structures with a pore size over 100 µm have been shown to allow for angiogenesis and the diffusion of oxygen and nutrients [40,41,359]. Although there is conflict in the literature on the optimal pore size [356], it has been shown that pore sizes between 300-900 µm result in higher and faster bone ingrowth [42,356]. Larger pores and higher porosity tend to improve mass transport due to increased permeability and diffusivity, allowing for cell diffusion, nutrient, waste, and growth factor transportation [351,355]. Similarly, topologically optimized concave surfaces have been shown to have higher rates of tissue deposition compared to flat or convex surfaces, along with higher permeability [359,360].

The effect of scaffold geometry on the biodegradation rate for load-bearing scaffolds is not well understood, with only one study to date having investigated it [361]. The biodegradation rate not only affects the time-dependent mechanical properties of the scaffold, but also the healing of the damaged tissue. Premature failure of the scaffold can result in too much load-transfer to the healing tissue causing necrosis [20]. Furthermore, control of the biodegradation rate ensures that the scaffold by-products are released at a sustainable rate that the body can safely metabolize. Li et al. were the first to investigate scaffold geometry specifically for BDM bone scaffolds by comparing 4 different scaffold designs based on a diamond unit cell as shown in Figure 10.

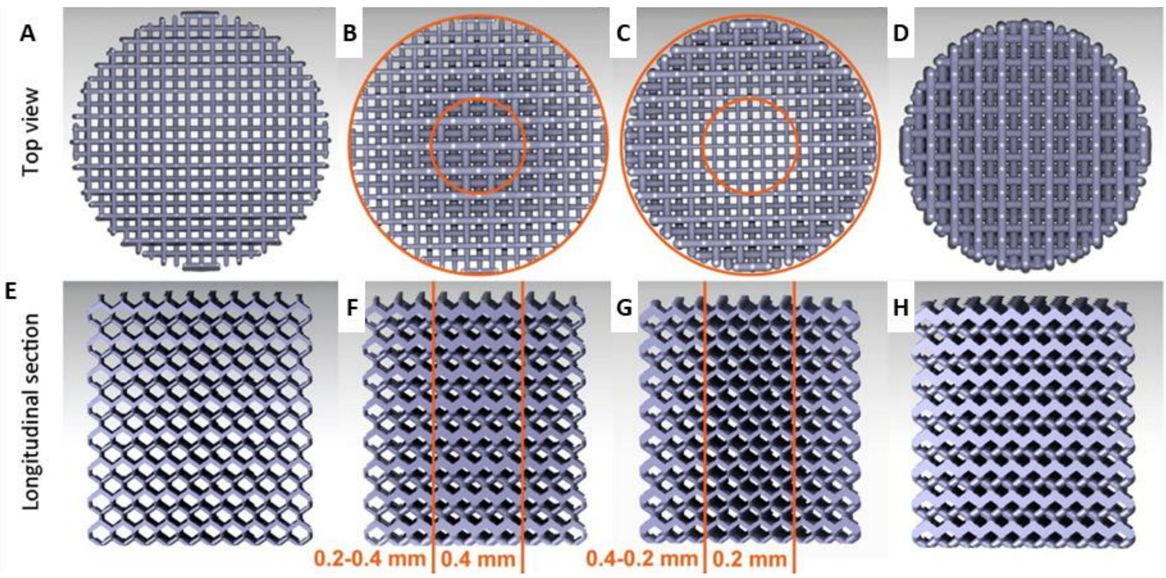

Figure 10 Four different scaffold designs based on diamond-unit cell: A,E) Uniform with a designed strut size of 200 μm, B,F) functionally graded with a denser center, C,G) functionally graded with a less dense center, D,H) uniform with a designed strut size of 400 μm. Reproduced with permission from [361].

It was found that the scaffold design significantly affected the permeability and subsequent biodegradation rate. As expected, the highly porous scaffold with a uniform strut size of 200μm had the highest degradation rate and permeability, along with the lowest mechanical properties. Conversely, the 400 μm scaffold had the highest mechanical properties and lowest fluid permeability and degradation rate. The graded scaffolds had comparable mechanical properties to each other, but the scaffold with a less dense center (Figure 10-C) had a higher degradation rate. This was attributed to the higher permeability and fluid flow in the center of the scaffold, resulting in a larger weight loss at the center of the scaffold compared to the outside. However, as mentioned previously, this did not seem to significantly affect the bulk mechanical properties of the scaffold, with both functionally graded scaffolds displaying mechanical properties approximately halfway between the 2 uniform struts both before and after immersion testing [361]. This study showed that scaffold geometry does play a critical role in the degradation rate, with further studies needing to investigate the effect of other variables (such as varying the unit cell design etc.) on the properties of BDM for load-bearing scaffold applications.

5.0 Future Recommendations

The selective laser melting of biodegradable metals is a novel research area with exciting possibilities that requires further exploration. The ability of SLM to create highly customizable bone scaffolds with intricate porous architecture to match the host bone morphology makes it an excellent candidate for manufacturing of biodegradable bone scaffold. Apart from overcoming the problems unique to each BDM family, additional challenges lay in the SLM processing of the material and the imparted properties in the final component. For Mg, its volatility and vaporization are key problems to address in future work. Similarly, with Zn, improving SLM process stability is key in manufacturing high quality scaffold. For these BDM, the challenge lies in process stabilization, partly through control of processing parameters, but also through modification of the processing atmosphere, pressure, and gas circulation. Lastly, Fe is a relatively easy biodegradable metal to manufacture using SLM; the challenge herein lies with improving the corrosion rate and bioactivity while maintaining, or improving, the mechanical properties.

There are currently no standards for testing the properties of BDM, let alone BDM for bone scaffold applications. As such, it can currently be difficult to directly compare the performance of BDM bone scaffolds in literature. Standardization of testing will allow for better comparison of scaffold performance to current clinical scaffolds, and to other BDM scaffolds. This is especially important for a highly versatile manufacturing technique, such as SLM, where multiple scaffold variables (e.g. scaffold geometry, material type, and hybrid materials) can be significantly modified, resulting in unique scaffolds. These unique scaffolds can be evaluated more efficiently and accurately with the help of standardized testing. Standardized testing will also allow for an easier transition into clinical trials and future commercialization of SLM manufacture BDM bone scaffolds.

To date there has only been one study on scaffold optimization and its effects on the mechanical, corrosion, and biological properties of SLM BDM bone scaffolds [361]. Previous studies have shown that scaffold architecture significantly affects not only the mechanical properties but also the cell attachment, proliferation, and *in vivo* healing rate [14,56]. Furthermore, scaffold architecture affects fluid permeability and the surface area exposed to the environment and, as such, can significantly affect the corrosion rate [351]. Post-processing of the scaffold can further affect the surface quality of the scaffold, which also requires further research. To this end, coatings and hybrid materials can help improve degradation rates and bioactivity [288,301], resulting in better implant integration. Future research should focus on the SLM of hybrid biodegradable materials and/or coatings of the scaffold. The effect of post-processing and finishing of the BDM scaffolds on its properties also requires further investigation. The combination of a complex geometry and a biodegradable alloy renders the conventional finishing methods, such as sand blasting or electropolishing difficult [298,332,362]. The removal of loose particles and improvement of the surface quality while maintaining dimensional accuracy requires further attention. Dimensional accuracy of these complex scaffolds before and after finishing steps call for the use of advanced techniques, such as computed x-ray tomography, both in terms of acquisition and analysis [363,364].

Alloy development for BDM bone scaffolds has been significantly studied and remains a hot topic of research; however, the effects of SLM on these alloys needs to be further investigated. To this point, research on lowering the cost of powder manufacturing is a concurrent research topic that needs further development if the research of SLM of BDM bone scaffolds is to evolve out of its early infancy. Ideally, novel alloy powders would be used for studies as opposed to mechanically alloying different powders together, yet the cost of the former is currently much too high. By exploring these challenges, SLM of BDM bone scaffolds will be an exciting field to keep an eye on.

Acknowledgments

DC, MJB, and MSD acknowledge the support of the School of Mechanical and Mining Engineering, the Queensland Centre for Advanced Materials Processing and Manufacturing, and the Australian Research Council Research Hub for Advanced Manufacturing of Medical Devices (IH150100024). AGD acknowledge the support of European Union, Repubblica Italiana, Regione Lombardia, and FESR for the project MADE4LO under the call "POR FESR 2014-2020 ASSE I - AZIONE I.1.B.1.3”. MJB also acknowledges the support of the Australian Research Council Discovery Program and is in receipt of Discover Early Career Researcher Award (DE160100260).

References

1) J.P. Schmitz and J.O. Hollinger, *Clinical orthopaedics and related research* 1986, pp. 299-308.

2) N.M. Haines, W.D. Lack, R.B. Seymour and M.J. Bosse, *Journal of orthopaedic trauma* 2016, vol. 30, pp. e158-63.

3) J.O. Hollinger and J.C. Kleinschmidt, *The Journal of craniofacial surgery* 1990, vol. 1, pp. 60-8.

4) United States Bone and Joint Initiative, (US Bone and Joint Initiative,: Rosemont, Illinois, 2016).

5) D.W. Hutmacher, *Biomaterials* 2000, vol. 21, pp. 2529-2543.

6) M. Niinomi, *Metallurgical and Materials Transactions A* 2002, vol. 33, p. 477.

7) X. Liu and P.X. Ma, *Annals of biomedical engineering* 2004, vol. 32, pp. 477-86.

8) A.R. Studart, U.T. Gonzenbach, E. Tervoort and L.J. Gauckler, *Journal of the American Ceramic Society* 2006, vol. 89, pp. 1771-1789.

9) W. Wang and K.W.K. Yeung, *Bioactive Materials* 2017, vol. 2, pp. 224-247.

10) C. Schwartz and R. Bordei, *European Journal of Orthopaedic Surgery & Traumatology* 2005, vol. 15, pp. 191-196.

11) R.D.A. Gaasbeek, H.G. Toonen, R.J. van Heerwaarden and P. Buma, *Biomaterials* 2005, vol. 26, pp. 6713-6719.

12) O. Böstman and H. Pihlajamäki, *Biomaterials* 2000, vol. 21, pp. 2615-2621.

13) P.V. Giannoudis, H. Dinopoulos and E. Tsiridis, *Injury* 2005, vol. 36, pp. S20-S27.

14) S. Van Bael, Y.C. Chai, S. Truscello, M. Moesen, G. Kerckhofs, H. Van Oosterwyck, J.P. Kruth and J. Schrooten, *Acta Biomaterialia* 2012, vol. 8, pp. 2824-2834.

15) G.E. Ryan, A.S. Pandit and D.P. Apatsidis, *Biomaterials* 2008, vol. 29, pp. 3625-3635.

16) M. Geetha, A.K. Singh, R. Asokamani and A.K. Gogia, *Progress in Materials Science* 2009, vol. 54, pp. 397-425.

17) T. Hanawa, *Materials Science and Engineering: C* 2004, vol. 24, pp. 745-752.

18) Y. Okazaki and E. Gotoh, *Corrosion Science* 2008, vol. 50, pp. 3429-3438.

19) Y. Okazaki and E. Gotoh, *Biomaterials* 2005, vol. 26, pp. 11-21.

20) Y.F. Zheng, X.N. Gu and F. Witte, *Materials Science and Engineering: R: Reports* 2014, vol. 77, pp. 1-34.

21) H. Li, Y. Zheng and L. Qin, *Progress in Natural Science: Materials International* 2014, vol. 24, pp. 414-422.

22) G. Ryan, A. Pandit and D.P. Apatsidis, *Biomaterials* 2006, vol. 27, pp. 2651-2670.

23) L.J. Gibson and M.F. Ashby: *Cellular solids: structure and properties*. (Cambridge university press, 1999).

24) S. Bose, S. Vahabzadeh and A. Bandyopadhyay, *Materials Today* 2013, vol. 16, pp. 496-504.

25) S.J. Hollister, *Nature Materials* 2005, vol. 4, pp. 518-524.

26) C. Mertens, H. Löwenheim and J. Hoffmann, *Journal of Cranio-Maxillofacial Surgery* 2013, vol. 41, pp. 219-225.

27) A.L. Jardini, M.A. Larosa, C.A. de Carvalho Zavaglia, L.F. Bernardes, C.S. Lambert, P. Kharmandayan, D. Calderoni and R. Maciel Filho, *Virtual and Physical Prototyping* 2014, vol. 9, pp. 115-125.

28) Y. Qin, P. Wen, H. Guo, D. Xia, Y. Zheng, L. Jauer, R. Poprawe, M. Voshage and J.H. Schleifenbaum, *Acta Biomaterialia* 2019, vol. 98, pp. 3-22.

29) A. Barone and U. Covani, *Journal of Oral and Maxillofacial Surgery* 2007, vol. 65, pp. 2039-2046.

30) A.A. Jahangir, ;, R.M. Nunley, S. Mehta and A. Sharan, *AAOS Now* 2008, vol. 2, pp. 35-37.

31) F. Chamieh, A.-M. Collignon, B.R. Coyac, J. Lesieur, S. Ribes, J. Sadoine, A. Llorens, A. Nicoletti, D. Letourneur, M.-L. Colombier, S.N. Nazhat, P. Bouchard, C. Chaussain and G.Y. Rochefort, 2016, vol. 6, p. 38814.

32) R.A. Kenley, K. Yim, J. Abrams, E. Ron, T. Turek, L.J. Marden and J.O. Hollinger, *Pharmaceutical Research* 1993, vol. 10, pp. 1393-1401.
33) J.S. Silber, D.G. Anderson, S.D. Daffner, B.T. Brislin, J.M. Leland, A.S. Hilibrand, A.R. Vaccaro and T.J. Albert, *Spine* 2003, vol. 28, pp. 134-9.
34) J.A. Goulet, L.E. Senunas, G.L. DeSilva and M.L. Greenfield, *Clinical orthopaedics and related research* 1997, pp. 76-81.
35) J. Older: *Bone implant grafting*. (Springer Science & Business Media, 2012).
36) E.R. Carlisle and J.S. Fischgrund, In *Surgical Management of Spinal Deformities*, ed. Thomas J. Errico, Lonner Baron S. and Moulton Andrew W. (W.B. Saunders: Philadelphia, 2009), pp 433-448.
37) J. Gleeson, N. Plunkett and F. O'Brien, *Eur Cell Mater* 2010, vol. 20, p. 30.
38) M. Navarro, A. Michiardi, O. Castaño and J.A. Planell, *Journal of the Royal Society Interface* 2008, vol. 5, pp. 1137-1158.
39) L. Roseti, V. Parisi, M. Petretta, C. Cavallo, G. Desando, I. Bartolotti and B. Grigolo, *Materials Science and Engineering: C* 2017, vol. 78, pp. 1246-1262.
40) S. Bose, M. Roy and A. Bandyopadhyay, *Trends in Biotechnology* 2012, vol. 30, pp. 546-554.
41) J. Rouwkema, N.C. Rivron and C.A. van Blitterswijk, *Trends in Biotechnology* 2008, vol. 26, pp. 434-441.
42) C.M. Murphy, M.G. Haugh and F.J. O'Brien, *Biomaterials* 2010, vol. 31, pp. 461-466.
43) D.F. Williams, *Biomaterials* 2008, vol. 29, pp. 2941-2953.
44) J.-Y. Rho, L. Kuhn-Spearing and P. Zioupos, *Medical Engineering & Physics* 1998, vol. 20, pp. 92-102.
45) K.A. Athanasiou, C. Zhu, D.R. Lanctot, C.M. Agrawal and X. Wang, *Tissue engineering* 2000, vol. 6, pp. 361-81.
46) L. Polo-Corrales, M. Latorre-Esteves and J.E. Ramirez-Vick, *Journal of nanoscience and nanotechnology* 2014, vol. 14, pp. 15-56.
47) A. Curodeau, E. Sachs and S. Caldarise, *Journal of biomedical materials research* 2000, vol. 53, pp. 525-35.
48) F.A. Shah, O. Omar, F. Suska, A. Snis, A. Matic, L. Emanuelsson, B. Norlindh, J. Lausmaa, P. Thomsen and A. Palmquist, *Acta Biomaterialia* 2016, vol. 36, pp. 296-309.
49) W. Zhang, X. Frank Walboomers, T.H. van Kuppevelt, W.F. Daamen, Z. Bian and J.A. Jansen, *Biomaterials* 2006, vol. 27, pp. 5658-5668.
50) J.P. Li, P. Habibovic, M. van den Doel, C.E. Wilson, J.R. de Wijn, C.A. van Blitterswijk and K. de Groot, *Biomaterials* 2007, vol. 28, pp. 2810-2820.
51) M.A. Lopez-Heredia, J. Sohier, C. Gaillard, S. Quillard, M. Dorget and P. Layrolle, *Biomaterials* 2008, vol. 29, pp. 2608-2615.
52) E.D. Spoerke, N.G. Murray, H. Li, L.C. Brinson, D.C. Dunand and S.I. Stupp, *Acta Biomaterialia* 2005, vol. 1, pp. 523-533.
53) F.A. Shah, A. Snis, A. Matic, P. Thomsen and A. Palmquist, *Acta Biomaterialia* 2016, vol. 30, pp. 357-367.
54) P.H. Warnke, T. Douglas, P. Wollny, E. Sherry, M. Steiner, S. Galonska, S.T. Becker, I.N. Springer, J. Wiltfang and S. Sivananthan, *Tissue engineering. Part C, Methods* 2009, vol. 15, pp. 115-24.
55) J. Van der Stok, P. Van der Jagt Olav, S. Amin Yavari, F.P. De Haas Mirthe, H. Waarsing Jan, H. Jahr, M.M. Van Lieshout Esther, P. Patka, A.N. Verhaar Jan, A. Zadpoor Amir and H. Weinans, *Journal of Orthopaedic Research* 2012, vol. 31, pp. 792-799.
56) N. Taniguchi, S. Fujibayashi, M. Takemoto, K. Sasaki, B. Otsuki, T. Nakamura, T. Matsushita, T. Kokubo and S. Matsuda, *Materials Science and Engineering: C* 2016, vol. 59, pp. 690-701.
57) J. Wieding, A. Jonitz and R. Bader, *Materials* 2012, vol. 5.
58) D.M. Robertson, L. Pierre and R. Chahal, *Journal of biomedical materials research* 1976, vol. 10, pp. 335-44.

59) W.C. Head, D.J. Bauk and R.H. Emerson, Jr., *Clinical orthopaedics and related research* 1995, pp. 85-90.
60) J.E. Davies, R. Matta, V.C. Mendes and P.S. Perri de Carvalho, *Organogenesis* 2010, vol. 6, pp. 161-6.
61) S. Yang, J. Wang, L. Tang, H. Ao, H. Tan, T. Tang and C. Liu, *Colloids and surfaces. B, Biointerfaces* 2014, vol. 116, pp. 72-80.
62) Y. Liu, Y. Zheng, X.-H. Chen, J.-A. Yang, H. Pan, D. Chen, L. Wang, J. Zhang, D. Zhu, S. Wu, K.W.K. Yeung, R.-C. Zeng, Y. Han and S. Guan, *Advanced Functional Materials* 2019, vol. 29, p. 1805402.
63) W. Maret, *International journal of molecular sciences* 2016, vol. 17.
64) S.S. Gropper and J.L. Smith: *Advanced nutrition and human metabolism*. (Cengage Learning, 2012).
65) H. Hermawan, *Progress in Biomaterials* 2018, vol. 7, pp. 93-110.
66) Y. Qin, P. Wen, H. Guo, D. Xia, Y. Zheng, L. Jauer, R. Poprawe, M. Voshage and J.H. Schleifenbaum, *Acta Biomaterialia* 2019.
67) F.I. Wolf and A. Cittadini, *Molecular Aspects of Medicine* 2003, vol. 24, pp. 3-9.
68) A. Hartwig, *Mutation Research/Fundamental and Molecular Mechanisms of Mutagenesis* 2001, vol. 475, pp. 113-121.
69) J. Vormann, *Molecular Aspects of Medicine* 2003, vol. 24, pp. 27-37.
70) N.-E.L. Saris, E. Mervaala, H. Karppanen, J.A. Khawaja and A. Lewenstam, *Clinica Chimica Acta* 2000, vol. 294, pp. 1-26.
71) F. Witte, *Acta Biomaterialia* 2015, vol. 23, pp. S28-S40.
72) M.P. Staiger, A.M. Pietak, J. Huadmai and G. Dias, *Biomaterials* 2006, vol. 27, pp. 1728-1734.
73) G. Song, *Corrosion Science* 2007, vol. 49, pp. 1696-1701.
74) Z. Qiao, Z. Shi, N. Hort, N.I. Zainal Abidin and A. Atrens, *Corrosion Science* 2012, vol. 61, pp. 185-207.
75) M.G. Seelig, *Archives of Surgery* 1924, vol. 8, pp. 669-680.
76) E. Andrews, *Journal of the American Medical Association* 1917, vol. LXIX, pp. 278-281.
77) F. Witte, V. Kaese, H. Haferkamp, E. Switzer, A. Meyer-Lindenberg, C.J. Wirth and H. Windhagen, *Biomaterials* 2005, vol. 26, pp. 3557-3563.
78) F. Witte, J. Fischer, J. Nellesen, H.-A. Crostack, V. Kaese, A. Pisch, F. Beckmann and H. Windhagen, *Biomaterials* 2006, vol. 27, pp. 1013-1018.
79) A. Purnama, H. Hermawan, J. Couet and D. Mantovani, *Acta Biomaterialia* 2010, vol. 6, pp. 1800-1807.
80) F. Witte, J. Fischer, J. Nellesen, C. Vogt, J. Vogt, T. Donath and F. Beckmann, *Acta Biomaterialia* 2010, vol. 6, pp. 1792-1799.
81) J. Kuhlmann, I. Bartsch, E. Willbold, S. Schuchardt, O. Holz, N. Hort, D. Hoche, W.R. Heineman and F. Witte, In *Acta Biomater*, (2012).
82) T. Kraus, S.F. Fischerauer, A.C. Hänzi, P.J. Uggowitzer, J.F. Löffler and A.M. Weinberg, *Acta Biomaterialia* 2012, vol. 8, pp. 1230-1238.
83) M. Salahshoor and Y. Guo, *Materials* 2012, vol. 5.
84) M.B. Kannan and R.K.S. Raman, *Biomaterials* 2008, vol. 29, pp. 2306-2314.
85) Y. Li, P.D. Hodgson and C.e. Wen, *Journal of Materials Science* 2011, vol. 46, pp. 365-371.
86) I.S. Berglund, H.S. Brar, N. Dolgova, A.P. Acharya, B.G. Keselowsky, M. Sarntinoranont and M.V. Manuel, *Journal of Biomedical Materials Research Part B: Applied Biomaterials* 2012, vol. 100B, pp. 1524-1534.
87) H. Du, Z. Wei, X. Liu and E. Zhang, *Materials Chemistry and Physics* 2011, vol. 125, pp. 568-575.
88) N.T. Kirkland, N. Birbilis, J. Walker, T. Woodfield, G.J. Dias and M.P. Staiger, *Journal of Biomedical Materials Research Part B: Applied Biomaterials* 2010, vol. 95B, pp. 91-100.
89) W.-C. Kim, J.-G. Kim, J.-Y. Lee and H.-K. Seok, *Materials Letters* 2008, vol. 62, pp. 4146-4148.

90) Y. Wan, G. Xiong, H. Luo, F. He, Y. Huang and X. Zhou, *Materials & Design* 2008, vol. 29, pp. 2034-2037.
91) Z. Li, X. Gu, S. Lou and Y. Zheng, *Biomaterials* 2008, vol. 29, pp. 1329-1344.
92) S. Zhang, X. Zhang, C. Zhao, J. Li, Y. Song, C. Xie, H. Tao, Y. Zhang, Y. He, Y. Jiang and Y. Bian, *Acta Biomaterialia* 2010, vol. 6, pp. 626-640.
93) Z.G. Huan, M.A. Leeflang, J. Zhou, L.E. Fratila-Apachitei and J. Duszczyk, *Journal of Materials Science: Materials in Medicine* 2010, vol. 21, pp. 2623-2635.
94) E. Zhang, W. He, H. Du and K. Yang, *Materials Science and Engineering: A* 2008, vol. 488, pp. 102-111.
95) E. Zhang, D. Yin, L. Xu, L. Yang and K. Yang, *Materials Science and Engineering: C* 2009, vol. 29, pp. 987-993.
96) B. Zhang, Y. Hou, X. Wang, Y. Wang and L. Geng, *Materials Science and Engineering: C* 2011, vol. 31, pp. 1667-1673.
97) H.S. Brar, J. Wong and M.V. Manuel, *Journal of the Mechanical Behavior of Biomedical Materials* 2012, vol. 7, pp. 87-95.
98) E. Zhang and L. Yang, *Materials Science and Engineering: A* 2008, vol. 497, pp. 111-118.
99) Y. Sun, B. Zhang, Y. Wang, L. Geng and X. Jiao, *Materials & Design* 2012, vol. 34, pp. 58-64.
100) F. Rosalbino, S. De Negri, A. Saccone, E. Angelini and S. Delfino, *Journal of materials science. Materials in medicine* 2010, vol. 21, pp. 1091-8.
101) B. Zhang, Y. Wang and L. Geng, In *Biomaterials-Physics and Chemistry*, (InTech: 2011).
102) X. Gu, Y. Zheng, Y. Cheng, S. Zhong and T. Xi, *Biomaterials* 2009, vol. 30, pp. 484-498.
103) E. Zhang, L. Yang, J. Xu and H. Chen, *Acta Biomaterialia* 2010, vol. 6, pp. 1756-1762.
104) Y. Li, C. Wen, D. Mushahary, R. Sravanthi, N. Harishankar, G. Pande and P. Hodgson, *Acta Biomaterialia* 2012, vol. 8, pp. 3177-3188.
105) Y.L. Zhou, J. An, D.M. Luo, W.Y. Hu, Y.C. Li, P. Hodgson and C.E. Wen, *Materials Technology* 2012, vol. 27, pp. 52-54.
106) W. Zhang, M. Li, Q. Chen, W. Hu, W. Zhang and W. Xin, *Materials & Design* 2012, vol. 39, pp. 379-383.
107) D. Mushahary, R. Sravanthi, Y. Li, M.J. Kumar, N. Harishankar, P.D. Hodgson, C. Wen and G. Pande, *International journal of nanomedicine* 2013, vol. 8, pp. 2887-902.
108) L. Mao, G. Yuan, J. Niu, Y. Zong and W. Ding, *Materials Science and Engineering: C* 2013, vol. 33, pp. 242-250.
109) L. Mao, G. Yuan, S. Wang, J. Niu, G. Wu and W. Ding, *Materials Letters* 2012, vol. 88, pp. 1-4.
110) Y. Zong, G. Yuan, X. Zhang, L. Mao, J. Niu and W. Ding, *Materials Science and Engineering: B* 2012, vol. 177, pp. 395-401.
111) X. Zhang, G. Yuan, J. Niu, P. Fu and W. Ding, *Journal of the Mechanical Behavior of Biomedical Materials* 2012, vol. 9, pp. 153-162.
112) X. Zhang, Y. Wu, Y. Xue, Z. Wang and L. Yang, *Materials Letters* 2012, vol. 86, pp. 42-45.
113) Z. Leng, J. Zhang, M. Zhang, X. Liu, H. Zhan and R. Wu, *Materials Science and Engineering: A* 2012, vol. 540, pp. 38-45.
114) X. Zhang, G. Yuan, L. Mao, J. Niu, P. Fu and W. Ding, *Journal of the Mechanical Behavior of Biomedical Materials* 2012, vol. 7, pp. 77-86.
115) Y. Chen, Z. Xu, C. Smith and J. Sankar, *Acta Biomaterialia* 2014, vol. 10, pp. 4561-4573.
116) F. Witte, N. Hort, C. Vogt, S. Cohen, K.U. Kainer, R. Willumeit and F. Feyerabend, *Current Opinion in Solid State and Materials Science* 2008, vol. 12, pp. 63-72.
117) N.I. Zainal Abidin, A.D. Atrens, D. Martin and A. Atrens, *Corrosion Science* 2011, vol. 53, pp. 3542-3556.
118) C. Wen, S. Guan, L. Peng, C. Ren, X. Wang and Z. Hu, *Applied Surface Science* 2009, vol. 255, pp. 6433-6438.
119) Y.M. Wang, F.H. Wang, M.J. Xu, B. Zhao, L.X. Guo and J.H. Ouyang, *Applied Surface Science* 2009, vol. 255, pp. 9124-9131.

120) X.N. Gu, W.R. Zhou, Y.F. Zheng, Y. Cheng, S.C. Wei, S.P. Zhong, T.F. Xi and L.J. Chen, *Acta Biomater* 2010, vol. 6, pp. 4605-13.

121) F. Witte, J. Fischer, J. Nellesen, H.A. Crostack, V. Kaese, A. Pisch, F. Beckmann and H. Windhagen, *Biomaterials* 2006, vol. 27, pp. 1013-8.

122) T. Zhang, Z. Xiang and F. Zhang, *Brachytherapy* 2016, vol. 15, p. S137.

123) F.-j. Zhang, C.-x. Li, G.-f. Duan, D. Chen and J.-j. Han, *Brachytherapy* 2011, vol. 10, p. S98.

124) W.D. Mueller, M.F. de Mele, M.L. Nascimento and M. Zeddies, *Journal of biomedical materials research. Part A* 2009, vol. 90, pp. 487-95.

125) M. Alvarez-Lopez, M.D. Pereda, J.A. del Valle, M. Fernandez-Lorenzo, M.C. Garcia-Alonso, O.A. Ruano and M.L. Escudero, *Acta Biomater* 2010, vol. 6, pp. 1763-71.

126) A. Pietak, P. Mahoney, G.J. Dias and M.P. Staiger, *Journal of materials science. Materials in medicine* 2008, vol. 19, pp. 407-15.

127) L. Bukovinová and B. Hadzima, *Corrosion Engineering, Science and Technology* 2012, vol. 47, pp. 352-357.

128) B. Hadzima, M. Mhaede and F. Pastorek, *Journal of Materials Science: Materials in Medicine* 2014, vol. 25, pp. 1227-1237.

129) B. Heublein, R. Rohde, V. Kaese, M. Niemeyer, W. Hartung and A. Haverich, *Heart (British Cardiac Society)* 2003, vol. 89, pp. 651-6.

130) F. Witte, H. Ulrich, M. Rudert and E. Willbold, *Journal of biomedical materials research. Part A* 2007, vol. 81, pp. 748-56.

131) O. Duygulu, R.A. Kaya, G. Oktay and A.A. Kaya, In *Materials science forum*, (Trans Tech Publ: 2007), pp 421-424.

132) H.M. Wong, K.W.K. Yeung, K.O. Lam, V. Tam, P.K. Chu, K.D.K. Luk and K.M.C. Cheung, *Biomaterials* 2010, vol. 31, p. 2084.

133) F. Witte, H. Ulrich, C. Palm and E. Willbold, *Journal of biomedical materials research. Part A* 2007, vol. 81, pp. 757-65.

134) Y. Song, D. Shan, R. Chen, F. Zhang and E.-H. Han, *Materials Science and Engineering: C* 2009, vol. 29, pp. 1039-1045.

135) Z. Wen, C. Wu, C. Dai and F. Yang, *Journal of Alloys and Compounds* 2009, vol. 488, pp. 392-399.

136) B. Venugopal and T.D. Luckey: *Metal toxicity in mammals. Volume 2. Chemical toxicity of metals and metalloids*. (Plenum Press., New York, N.Y., 1978).

137) Y. Ding, C. Wen, P. Hodgson and Y. Li, *Journal of Materials Chemistry B* 2014, vol. 2, pp. 1912-1933.

138) P.C. Ferreira, A. Piai Kde, A.M. Takayanagui and S.I. Segura-Munoz, *Revista latino-americana de enfermagem* 2008, vol. 16, pp. 151-7.

139) M. Shingde, J. Hughes, R. Boadle, E.J. Wills and R. Pamphlett, *The Medical journal of Australia* 2005, vol. 183, pp. 145-6.

140) A.V. Rousselle, D. Heymann, V. Demais, C. Charrier, N. Passuti and M.F. Basle, *Histology and histopathology* 2002, vol. 17, pp. 1025-32.

141) H. Sigel: *Metal Ions in Biological Systems: Volume 40: The Lanthanides and Their Interrelations with Biosystems*. (CRC Press, 2003).

142) H.G. Seiler, H. Sigel and A. Sigel: *Handbook on toxicity of inorganic compounds*. (Marcel Dekker,New York, NY, United States, 1988).

143) C. Di Mario, H.U.W. Griffiths, O. Goktekin, N. Peeters, J.A.N. Verbist, M. Bosiers, K. Deloose, B. Heublein, R. Rohde, V. Kasese, C. Ilsley and R. Erbel, *Journal of Interventional Cardiology* 2004, vol. 17, pp. 391-395.

144) T.L.P. Slottow, R. Pakala, T. Okabe, D. Hellinga, R.J. Lovec, F.O. Tio, A.B. Bui and R. Waksman, *Cardiovascular Revascularization Medicine* 2008, vol. 9, pp. 248-254.

145) R. Waksman, R. Pakala, P.K. Kuchulakanti, R. Baffour, D. Hellinga, R. Seabron, F.O. Tio, E. Wittchow, S. Hartwig, C. Harder, R. Rohde, B. Heublein, A. Andreae, K.-H. Waldmann and A. Haverich, *Catheterization and Cardiovascular Interventions* 2006, vol. 68, pp. 607-617.

146) M. Haude, R. Erbel, P. Erne, S. Verheye, H. Degen, D. Böse, P. Vermeersch, I. Wijnbergen, N. Weissman, F. Prati, R. Waksman and J. Koolen, *The Lancet* 2013, vol. 381, pp. 836-844.

147) R. Erbel, C. Di Mario, J. Bartunek, J. Bonnier, B. de Bruyne, F.R. Eberli, P. Erne, M. Haude, B. Heublein, M. Horrigan, C. Ilsley, D. Böse, J. Koolen, T.F. Lüscher, N. Weissman and R. Waksman, *The Lancet* 2007, vol. 369, pp. 1869-1875.

148) R. Waksman, R. Erbel, C. Di Mario, J. Bartunek, B. de Bruyne, F.R. Eberli, P. Erne, M. Haude, M. Horrigan, C. Ilsley, D. Böse, H. Bonnier, J. Koolen, T.F. Lüscher and N.J. Weissman, *JACC: Cardiovascular Interventions* 2009, vol. 2, pp. 312-320.

149) P. Barlis, J. Tanigawa and C. Di Mario, *European Heart Journal* 2007, vol. 28, pp. 2319-2319.

150) M. Bosiers, K. Deloose, J. Verbist and P. Peeters, *The Journal of cardiovascular surgery* 2006, vol. 47, pp. 171-6.

151) P. Peeters, M. Bosiers, J. Verbist, K. Deloose and B. Heublein, *Journal of Endovascular Therapy* 2005, vol. 12, pp. 1-5.

152) P. Zartner, M. Buettner, H. Singer and M. Sigler, *Catheterization and Cardiovascular Interventions* 2007, vol. 69, pp. 443-446.

153) D. Schranz, P. Zartner, I. Michel-Behnke and H. Akintürk, *Catheterization and Cardiovascular Interventions* 2006, vol. 67, pp. 671-673.

154) P. Zartner, R. Cesnjevar, H. Singer and M. Weyand, *Catheterization and Cardiovascular Interventions* 2005, vol. 66, pp. 590-594.

155) Syntellix;, "MAGNEZIX®" (2017), http://www.syntellix.de/en/home.html ccessed Access Date Access Year|.

156) H. Windhagen, K. Radtke, A. Weizbauer, J. Diekmann, Y. Noll, U. Kreimeyer, R. Schavan, C. Stukenborg-Colsman and H. Waizy, *BioMedical Engineering OnLine* 2013, vol. 12, p. 62.

157) R. Biber, J. Pauser, Ge, #xdf, M. lein and H.J. Bail, *Case Reports in Orthopedics* 2016, vol. 2016, p. 4.

158) D. Zhao, S. Huang, F. Lu, B. Wang, L. Yang, L. Qin, K. Yang, Y. Li, W. Li, W. Wang, S. Tian, X. Zhang, W. Gao, Z. Wang, Y. Zhang, X. Xie, J. Wang and J. Li, *Biomaterials* 2016, vol. 81, pp. 84-92.

159) J.-W. Lee, H.-S. Han, K.-J. Han, J. Park, H. Jeon, M.-R. Ok, H.-K. Seok, J.-P. Ahn, K.E. Lee, D.-H. Lee, S.-J. Yang, S.-Y. Cho, P.-R. Cha, H. Kwon, T.-H. Nam, J.H.L. Han, H.-J. Rho, K.-S. Lee, Y.-C. Kim and D. Mantovani, *Proceedings of the National Academy of Sciences* 2016, vol. 113, p. 716.

160) A.H. Yusop, A.A. Bakir, N.A. Shaharom, M.R. Abdul Kadir and H. Hermawan, *International Journal of Biomaterials* 2012, vol. 2012, p. 10.

161) L.P. Lefebvre, J. Banhart and D.C. Dunand, *Advanced Engineering Materials* 2008, vol. 10, pp. 775-787.

162) R. Narayan, V. Burt, S. Lampman, K. Marken, E. Marquard and B. Riley, *Materials for Medical Devices; ASM International: Materials Park, OH, USA* 2012, vol. 23.

163) C.E. Wen, Y. Yamada, K. Shimojima, Y. Chino, H. Hosokawa and M. Mabuchi, *Materials Letters* 2004, vol. 58, pp. 357-360.

164) H. Zhuang, Y. Han and A. Feng, *Materials Science and Engineering: C* 2008, vol. 28, pp. 1462-1466.

165) R. Ma, Y.-x. Lai, L. Li, H.-l. Tan, J.-l. Wang, Y. Li, T.-t. Tang and L. Qin, *Scientific Reports* 2015, vol. 5, p. 13775.

166) Y. Lai, L. Li, S. Chen, M. Zhang, X. Wang, P. Zhang and L. Qin, *Journal of Orthopaedic Translation* 2014, vol. 2, pp. 218-219.

167) D. Zhao, F. Witte, F. Lu, J. Wang, J. Li and L. Qin, *Biomaterials* 2017, vol. 112, pp. 287-302.

168) H. Tapiero and K.D. Tew, *Biomedicine & Pharmacotherapy* 2003, vol. 57, pp. 399-411.

169) M. Hambidge, *The Journal of nutrition* 2000, vol. 130, pp. 1344S-1349S.

170) E. Mostaed, M. Sikora-Jasinska, J.W. Drelich and M. Vedani, *Acta Biomaterialia* 2018, vol. 71, pp. 1-23.
171) J. Venezuela and M.S. Dargusch, *Acta Biomaterialia* 2019, vol. 87, pp. 1-40.
172) P. Trumbo, S. Schlicker, A.A. Yates and M. Poos, *Journal of the American Dietetic Association* 2002, vol. 102, pp. 1621-1630.
173) G.J. Fosmire, *The American journal of clinical nutrition* 1990, vol. 51, pp. 225-7.
174) C.J. Frederickson, J.-Y. Koh and A.I. Bush, *Nature Reviews Neuroscience* 2005, vol. 6, pp. 449-462.
175) B.D. Ratner, A.S. Hoffman, F.J. Schoen and J.E. Lemons, In *Biomaterials Science (Third Edition)*, ed. Buddy D. Ratner, Hoffman Allan S., Schoen Frederick J. and Lemons Jack E. (Academic Press: 2013), pp xli-liii.
176) P.K. Bowen, J. Drelich and J. Goldman, *Advanced Materials* 2013, vol. 25, pp. 2577-2582.
177) P.K. Bowen, E.R. Shearier, S. Zhao, R.J. Guillory, F. Zhao, J. Goldman and J.W. Drelich, *Advanced Healthcare Materials* 2016, vol. 5, pp. 1121-1140.
178) H. Gong, K. Wang, R. Strich and J.G. Zhou, *Journal of Biomedical Materials Research - Part B Applied Biomaterials* 2015, vol. 103, pp. 1632-1640.
179) C. Yao, Z. Wang, S.L. Tay, T. Zhu and W. Gao, *Journal of Alloys and Compounds* 2014, vol. 602, pp. 101-107.
180) H. Li, H. Yang, Y. Zheng, F. Zhou, K. Qiu and X. Wang, *Materials and Design* 2015, vol. 83, pp. 95-102.
181) J. Kubásek, D. Vojtěch, E. Jablonská, I. Pospíšilová, J. Lipov and T. Ruml, *Materials Science and Engineering C* 2016, vol. 58, pp. 24-35.
182) M.S. Dambatta, S. Izman, D. Kurniawan, S. Farahany, B. Yahaya and H. Hermawan, *Materials & Design* 2015, vol. 85, pp. 431-437.
183) D. Vojtěch, J. Kubásek, J. Šerák and P. Novák, *Acta Biomaterialia* 2011, vol. 7, pp. 3515-3522.
184) H.F. Li, X.H. Xie, Y.F. Zheng, Y. Cong, F.Y. Zhou, K.J. Qiu, X. Wang, S.H. Chen, L. Huang, L. Tian and L. Qin, 2015, vol. 5, p. 10719.
185) J. Niu, Z. Tang, H. Huang, J. Pei, H. Zhang, G. Yuan and W. Ding, *Materials Science and Engineering C* 2016, vol. 69, pp. 407-413.
186) Z. Tang, H. Huang, J. Niu, L. Zhang, H. Zhang, J. Pei, J. Tan and G. Yuan, *Materials & Design* 2017, vol. 117, pp. 84-94.
187) S. Zhao, J.-M. Seitz, R. Eifler, H.J. Maier, R.J. Guillory, E.J. Earley, A. Drelich, J. Goldman and J.W. Drelich, *Materials Science and Engineering: C* 2017, vol. 76, pp. 301-312.
188) S. Zhao, C.T. McNamara, P.K. Bowen, N. Verhun, J.P. Braykovich, J. Goldman and J.W. Drelich, *Metallurgical and Materials Transactions A* 2017, vol. 48, pp. 1204-1215.
189) S. Sun, Y. Ren, L. Wang, B. Yang, H. Li and G. Qin, *Materials Science and Engineering: A* 2017, vol. 701, pp. 129-133.
190) P. Sotoudeh Bagha, S. Khaleghpanah, S. Sheibani, M. Khakbiz and A. Zakeri, *Journal of Alloys and Compounds* 2018, vol. 735, pp. 1319-1327.
191) M. Sikora-Jasinska, E. Mostaed, A. Mostaed, R. Beanland, D. Mantovani and M. Vedani, *Materials Science and Engineering: C* 2017, vol. 77, pp. 1170-1181.
192) P. Li, C. Schille, E. Schweizer, F. Rupp, A. Heiss, C. Legner, U.E. Klotz, J. Geis-Gerstorfer and L. Scheideler, *International journal of molecular sciences* 2018, vol. 19.
193) H.F. Li, X.H. Xie, Y.F. Zheng, Y. Cong, F.Y. Zhou, K.J. Qiu, X. Wang, S.H. Chen, L. Huang, L. Tian and L. Qin, *Scientific Reports* 2015, vol. 5, p. 10719.
194) C. Xiao, L. Wang, Y. Ren, S. Sun, E. Zhang, C. Yan, Q. Liu, X. Sun, F. Shou, J. Duan, H. Wang and G. Qin, *Journal of Materials Science & Technology* 2018, vol. 34, pp. 1618-1627.
195) H. Yang, X. Qu, W. Lin, C. Wang, D. Zhu, K. Dai and Y. Zheng, *Acta Biomaterialia* 2018, vol. 71, pp. 200-214.
196) L. Zhao, Z. Zhang, Y. Song, S. Liu, Y. Qi, X. Wang, Q. Wang and C. Cui, *Materials & Design* 2016, vol. 108, pp. 136-144.

197) J. Čapek, E. Jablonská, J. Lipov, T.F. Kubatík and D. Vojtěch, *Materials Chemistry and Physics* 2018, vol. 203, pp. 249-258.
198) Y. Hou, G. Jia, R. Yue, C. Chen, J. Pei, H. Zhang, H. Huang, M. Xiong and G. Yuan, *Materials Characterization* 2018, vol. 137, pp. 162-169.
199) L. Zhao, Y. Xie, Z. Zhang, X. Wang, Y. Qi, T. Wang, R. Wang and C. Cui, *Materials Characterization* 2018, vol. 144, pp. 227-238.
200) Y. Xie, L. Zhao, Z. Zhang, X. Wang, R. Wang and C. Cui, *Materials Chemistry and Physics* 2018, vol. 219, pp. 433-443.
201) J. Čapek, J. Pinc, Š. Msallamová, E. Jablonská, P. Veřtát, J. Kubásek and D. Vojtěch, *Journal of Thermal Spray Technology* 2019, vol. 28, pp. 826-841.
202) L. Zhao, X. Wang, T. Wang, Y. Xia and C. Cui, *Materials Letters* 2019, vol. 247, pp. 75-78.
203) L.J. Gibson and M.F. Ashby: *Cellular solids : structure and properties*. 2nd ed., 1st pbk. ed. with corr.. ed. (Cambridge : Cambridge University Press, 1999).
204) G. Papanikolaou and K. Pantopoulos, *Toxicology and Applied Pharmacology* 2005, vol. 202, pp. 199-211.
205) H.K. Lim, J.L. Riddell, A.C. Nowson, O.A. Booth and A.E. Szymlek-Gay, *Nutrients* 2013, vol. 5.
206) E. Crubzy, P. Murail, L. Girard and J.-P. Bernadou, *Nature* 1998, vol. 391, pp. 29-29.
207) A.A. Zierold, *Archives of Surgery* 1924, vol. 9, pp. 365-412.
208) M. Peuster, P. Wohlsein, M. Brügmann, M. Ehlerding, K. Seidler, C. Fink, H. Brauer, A. Fischer and G. Hausdorf, *Heart* 2001, vol. 86, p. 563.
209) H. Hermawan, D. Dubé and D. Mantovani, *Journal of Biomedical Materials Research Part A* 2010, vol. 93A, pp. 1-11.
210) R. Waksman, R. Pakala, R. Baffour, R. Seabron, D. Hellinga and F.O. Tio, *J Interv Cardiol* 2008, vol. 21, pp. 15-20.
211) M. Peuster, C. Hesse, T. Schloo, C. Fink, P. Beerbaum and C. von Schnakenburg, *Biomaterials* 2006, vol. 27, pp. 4955-4962.
212) B. Liu and Y.F. Zheng, *Acta Biomater* 2011, vol. 7, pp. 1407-20.
213) H. Wang, Y. Zheng, J. Liu, C. Jiang and Y. Li, *Materials Science and Engineering: C* 2017, vol. 71, pp. 60-66.
214) J. Čapek, K. Stehlíková, A. Michalcová, Š. Msallamová and D. Vojtěch, *Materials Chemistry and Physics* 2016, vol. 181, pp. 501-511.
215) T. Huang, J. Cheng, D. Bian and Y. Zheng, *Journal of Biomedical Materials Research Part B: Applied Biomaterials* 2016, vol. 104, pp. 225-240.
216) T. Huang, J. Cheng and Y.F. Zheng, *Materials Science and Engineering: C* 2014, vol. 35, pp. 43-53.
217) J. He, F.-L. He, D.-W. Li, Y.-L. Liu, Y.-Y. Liu, Y.-J. Ye and D.-C. Yin, *RSC Advances* 2016, vol. 6, pp. 112819-112838.
218) B. Wegener, B. Sievers, S. Utzschneider, P. Müller, V. Jansson, S. Rößler, B. Nies, G. Stephani, B. Kieback and P. Quadbeck, *Materials Science and Engineering: B* 2011, vol. 176, pp. 1789-1796.
219) J.H. Beattie and A. Avenell, *Nutrition research reviews* 1992, vol. 5, pp. 167-88.
220) M. Schinhammer, A.C. Hänzi, J.F. Löffler and P.J. Uggowitzer, *Acta Biomaterialia* 2010, vol. 6, pp. 1705-1713.
221) M.S. Dargusch, A. Dehghan-Manshadi, M. Shahbazi, J. Venezuela, X. Tran, J. Song, N. Liu, C. Xu, Q. Ye and C. Wen, *ACS Biomaterials Science & Engineering* 2019, vol. 5, pp. 1686-1702.
222) H. Hermawan, H. Alamdari, D. Mantovani and D. Dubé, *Powder Metallurgy* 2008, vol. 51, pp. 38-45.
223) H. Hermawan, D. Dubé and D. Mantovani, In *Advanced Materials Research*, (Trans Tech Publ: 2007), pp 107-112.
224) H. Hermawan, A. Purnama, D. Dube, J. Couet and D. Mantovani, *Acta biomaterialia* 2010, vol. 6, pp. 1852-60.

225) H. Hermawan, D. Dube and D. Mantovani, *Journal of biomedical materials research. Part A* 2010, vol. 93, pp. 1-11.
226) M. Schinhammer, P. Steiger, F. Moszner, J.F. Löffler and P.J. Uggowitzer, *Materials Science and Engineering: C* 2013, vol. 33, pp. 1882-1893.
227) H. Hermawan, A. Purnama, D. Dube, J. Couet and D. Mantovani, *Acta Biomaterialia* 2010, vol. 6, pp. 1852-1860.
228) Q. Zhang and P. Cao, *Materials Chemistry and Physics* 2015, vol. 163, pp. 394-401.
229) J. Čapek, J. Kubásek, D. Vojtěch, E. Jablonská, J. Lipov and T. Ruml, *Materials Science and Engineering: C* 2016, vol. 58, pp. 900-908.
230) B. Liu, Y.F. Zheng and L. Ruan, *Materials Letters* 2011, vol. 65, pp. 540-543.
231) O. Bouaziz, S. Allain, C.P. Scott, P. Cugy and D. Barbier, *Current Opinion in Solid State and Materials Science* 2011, vol. 15, pp. 141-168.
232) M. Schinhammer, C.M. Pecnik, F. Rechberger, A.C. Hänzi, J.F. Löffler and P.J. Uggowitzer, *Acta Materialia* 2012, vol. 60, pp. 2746-2756.
233) T. Kraus, F. Moszner, S. Fischerauer, M. Fiedler, E. Martinelli, J. Eichler, F. Witte, E. Willbold, M. Schinhammer, M. Meischel, P.J. Uggowitzer, J.F. Löffler and A. Weinberg, *Acta Biomaterialia* 2014, vol. 10, pp. 3346-3353.
234) S. Loffredo, C. Paternoster, N. Giguère, G. Barucca, M. Vedani and D. Mantovani, *Acta Biomaterialia* 2019, vol. 98, pp. 103-113.
235) R. Gorejová, L. Haverová, R. Oriňaková, A. Oriňak and M. Oriňak, *Journal of Materials Science* 2019, vol. 54, pp. 1913-1947.
236) F. Zivic, N. Grujovic, E. Pellicer, J. Sort, S. Mitrovic, D. Adamovic and M. Vulovic, In *Biomaterials in Clinical Practice : Advances in Clinical Research and Medical Devices*, ed. Fatima Zivic, Affatato Saverio, Trajanovic Miroslav, Schnabelrauch Matthias, Grujovic Nenad and Choy Kwang Leong (Springer International Publishing: Cham, 2018), pp 225-280.
237) American Society for Testing and Materials, (ASTM,: 2015).
238) S. Meteyer, X. Xu, N. Perry and Y.F. Zhao, *Procedia CIRP* 2014, vol. 15, pp. 19-25.
239) X. Xu, S. Meteyer, N. Perry and Y.F. Zhao, *International Journal of Production Research* 2015, vol. 53, pp. 7005-7015.
240) K.V. Wong and A. Hernandez, *ISRN Mechanical Engineering* 2012, vol. 2012, p. 10.
241) P.K. Gokuldoss, S. Kolla and J. Eckert, *Materials* 2017, vol. 10, p. 672.
242) D.T. Chou, D. Wells, D. Hong, B. Lee, H. Kuhn and P.N. Kumta, *Acta Biomaterialia* 2013, vol. 9, pp. 8593-8603.
243) D. Hong, D.-T. Chou, O.I. Velikokhatnyi, A. Roy, B. Lee, I. Swink, I. Issaev, H.A. Kuhn and P.N. Kumta, *Acta Biomaterialia* 2016, vol. 45, pp. 375-386.
244) A. Mostafaei, E.L. Stevens, E.T. Hughes, S.D. Biery, C. Hilla and M. Chmielus, *Materials & Design* 2016, vol. 108, pp. 126-135.
245) C. Yang, Z. Huan, X. Wang, C. Wu and J. Chang, *ACS Biomaterials Science & Engineering* 2018, vol. 4, pp. 608-616.
246) H. Attar, K.G. Prashanth, A.K. Chaubey, M. Calin, L.C. Zhang, S. Scudino and J. Eckert, *Materials Letters* 2015, vol. 142, pp. 38-41.
247) K.G. Prashanth, B. Debalina, Z. Wang, P.F. Gostin, A. Gebert, M. Calin, U. Kühn, M. Kamaraj, S. Scudino and J. Eckert, *Journal of Materials Research* 2014, vol. 29, pp. 2044-2054.
248) K.G. Prashanth, S. Scudino and J. Eckert, *Acta Materialia* 2017, vol. 126, pp. 25-35.
249) C.E. Wen, Y. Yamada, K. Shimojima, Y. Chino, H. Hosokawa and M. Mabuchi, In *Materials Science Forum*, (Trans Tech Publ: 2003), pp 1001-1006.
250) C.E. Wen, M. Mabuchi, Y. Yamada, K. Shimojima, Y. Chino and T. Asahina, *Scripta Materialia* 2001, vol. 45, pp. 1147-1153.
251) Z.S. Seyedraoufi and S. Mirdamadi, *Journal of the Mechanical Behavior of Biomedical Materials* 2013, vol. 21, pp. 1-8.

252) M.P. Staiger, I. Kolbeinsson, N.T. Kirkland, T. Nguyen, G. Dias and T.B.F. Woodfield, *Materials Letters* 2010, vol. 64, pp. 2572-2574.

253) N.T. Kirkland, I. Kolbeinsson, T. Woodfield, G.J. Dias and M.P. Staiger, *Materials Science and Engineering: B* 2011, vol. 176, pp. 1666-1672.

254) F. Geng, L. Tan, B. Zhang, C. Wu, Y. He, J. Yang and K. Yang, *Journal of Materials Science and Technology* 2009, vol. 25, pp. 123-129.

255) V. Manakari, G. Parande and M. Gupta, *Metals* 2017, vol. 7.

256) M.M. Savalani, C.C. Ng and H.C. Man, In *2010 International Conference on Manufacturing Automation*, (2010), pp 50-54.

257) C.C. Ng, M.M. Savalani, H.C. Man and I. Gibson, *Virtual and Physical Prototyping* 2010, vol. 5, pp. 13-19.

258) C.C. Ng, M.M. Savalani and H.C. Man, *Rapid Prototyping Journal* 2011, vol. 17, pp. 479-490.

259) C.C. Ng, M.M. Savalani, M.L. Lau and H.C. Man, *Applied Surface Science* 2011, vol. 257, pp. 7447-7454.

260) B. Zhang, H. Liao and C. Coddet, *Materials & Design* 2012, vol. 34, pp. 753-758.

261) A. International, A.I.H. Committee and A.I.A.P.D. Committee: *Metals Handbook: Properties and selection*. (Asm International, 1990).

262) K. Wei, M. Gao, Z. Wang and X. Zeng, *Materials Science and Engineering: A* 2014, vol. 611, pp. 212-222.

263) D. Schmid, J. Renza, M.F. Zaeh and J. Glasschroeder, *Physics Procedia* 2016, vol. 83, pp. 927-936.

264) K. Wei, Z. Wang and X. Zeng, *Materials Letters* 2015, vol. 156, pp. 187-190.

265) K. Wei, X. Zeng, Z. Wang, J. Deng, M. Liu, G. Huang and X. Yuan, *Materials Science and Engineering: A* 2019, vol. 756, pp. 226-236.

266) M. Gieseke, C. Noelke, S. Kaierle, V. Wesling and H. Haferkamp, In *Magnesium Technology 2013*, ed. Norbert Hort, Mathaudhu Suveen Nigel, Neelameggham Neale R. and Alderman Martyn (Springer International Publishing: Cham, 2016), pp 65-68.

267) M. Gieseke, C. Nölke, S. Kaierle, H. J. Maier and H. Haferkamp, In *International Conference of Biomedical Technology*, (Hannover, 2013).

268) D. Hu, Y. Wang, D. Zhang, L. Hao, J. Jiang, Z. Li and Y. Chen, *Materials and Manufacturing Processes* 2015, vol. 30, pp. 1298-1304.

269) S. Monica Mahesh and P. Jorge Martinez, *Rapid Prototyping Journal* 2016, vol. 22, pp. 115-122.

270) Y. Yang, P. Wu, X. Lin, Y. Liu, H. Bian, Y. Zhou, C. Gao and C. Shuai, *Virtual and Physical Prototyping* 2016, vol. 11, pp. 173-181.

271) Y. Yang, P. Wu, Q. Wang, H. Wu, Y. Liu, Y. Deng, Y. Zhou and C. Shuai, *Materials* 2016, vol. 9.

272) J. Chen, P. Wu, Q. Wang, Y. Yang, S. Peng, Y. Zhou, C. Shuai and Y. Deng, *Metals* 2016, vol. 6.

273) Y. Zhou, P. Wu, Y. Yang, D. Gao, P. Feng, C. Gao, H. Wu, Y. Liu, H. Bian and C. Shuai, *Journal of Alloys and Compounds* 2016, vol. 687, pp. 109-114.

274) C. Shuai, Y. Yang, P. Wu, X. Lin, Y. Liu, Y. Zhou, P. Feng, X. Liu and S. Peng, *Journal of Alloys and Compounds* 2017, vol. 691, pp. 961-969.

275) C. Shuai, Y. Zhou, X. Lin, Y. Yang, C. Gao, X. Shuai, H. Wu, X. Liu, P. Wu and P. Feng, *Journal of Materials Science: Materials in Medicine* 2016, vol. 28, p. 13.

276) T. Long, X. Zhang, Q. Huang, L. Liu, Y. Liu, J. Ren, Y. Yin, D. Wu and H. Wu, *Virtual and Physical Prototyping* 2018, vol. 13, pp. 71-81.

277) K. Ralston and N. Birbilis, *Corrosion* 2010, vol. 66, pp. 075005-075005-13.

278) C. Shuai, Y. Zhou, Y. Yang, P. Feng, L. Liu, C. He, M. Zhao, S. Yang, C. Gao and P. Wu, *Materials* 2017, vol. 10.

279) H.-M. Kim, T. Himeno, T. Kokubo and T. Nakamura, *Biomaterials* 2005, vol. 26, pp. 4366-4373.

280) Y. Deng, Y. Yang, C. Gao, P. Feng, W. Guo, C. He, J. Chen and C. Shuai, *International Journal of Bioprinting; Vol 4, No 1 (2018)* 2018.
281) J. Matena, S. Petersen, M. Gieseke, M. Teske, M. Beyerbach, A. Kampmann, H. Murua Escobar, N.C. Gellrich, H. Haferkamp and I. Nolte, *International journal of molecular sciences* 2015, vol. 16, pp. 13287-301.
282) L. Jauer, B. Jülich, M. Voshage and W. Meiners, *European Cells Materials* 2015, vol. 30, p. 1.
283) C. Liu, M. Zhang and C. Chen, *Materials Science and Engineering: A* 2017, vol. 703, pp. 359-371.
284) Y. Li, J. Zhou, P. Pavanram, M.A. Leeflang, L.I. Fockaert, B. Pouran, N. Tümer, K.U. Schröder, J.M.C. Mol, H. Weinans, H. Jahr and A.A. Zadpoor, *Acta Biomaterialia* 2018, vol. 67, pp. 378-392.
285) A. Kopp, T. Derra, M. Müther, L. Jauer, J.H. Schleifenbaum, M. Voshage, O. Jung, R. Smeets and N. Kröger, *Acta Biomaterialia* 2019, vol. 98, pp. 23-35.
286) L. Jauer, W. Meiners, S. Vervoort, C. Gayer, N.A. Zumdick and D. Zander, In *European Congress and Exhibition on Powder Metallurgy. European PM Conference Proceedings*, (The European Powder Metallurgy Association: 2016), pp 1-6.
287) F. Witte, L. Jauer, W. Meiners, Z. Kronbach, K. Strohschein and T. Schmidt, *Front. Bioeng. Biotechnol.* 2016, vol. 4.
288) J. Matena, S. Petersen, M. Gieseke, M. Teske, M. Beyerbach, A. Kampmann, M.H. Escobar, N.-C. Gellrich, H. Haferkamp and I. Nolte, *International Journal of Molecular Sciences* 2015, vol. 16.
289) Y. Li, H. Jahr, X.Y. Zhang, M.A. Leeflang, W. Li, B. Pouran, F.D. Tichelaar, H. Weinans, J. Zhou and A.A. Zadpoor, *Additive Manufacturing* 2019, vol. 28, pp. 299-311.
290) M. Montani, A.G. Demir, E. Mostaed, M. Vedani and B. Previtali, *Rapid Prototyping Journal* 2017, vol. 23, pp. 514-523.
291) A.G. Demir, L. Monguzzi and B. Previtali, *Additive Manufacturing* 2017, vol. 15, pp. 20-28.
292) P. Wen, L. Jauer, M. Voshage, Y. Chen, R. Poprawe and J.H. Schleifenbaum, *Journal of Materials Processing Technology* 2018, vol. 258, pp. 128-137.
293) P. Wen, M. Voshage, L. Jauer, Y. Chen, Y. Qin, R. Poprawe and J.H. Schleifenbaum, *Materials & Design* 2018, vol. 155, pp. 36-45.
294) C. Shuai, L. Xue, C. Gao, Y. Yang, S. Peng and Y. Zhang, *Virtual and Physical Prototyping* 2018, vol. 13, pp. 146-154.
295) Y. Yang, F. Yuan, C. Gao, P. Feng, L. Xue, S. He and C. Shuai, *Journal of the Mechanical Behavior of Biomedical Materials* 2018, vol. 82, pp. 51-60.
296) C. Shuai, Y. Cheng, Y. Yang, S. Peng, W. Yang and F. Qi, *Journal of Alloys and Compounds* 2019, vol. 798, pp. 606-615.
297) A.G. Demir and B. Previtali, *Materials & Design* 2017, vol. 119, pp. 338-350.
298) P. Wen, Y. Qin, Y. Chen, M. Voshage, L. Jauer, R. Poprawe and J.H. Schleifenbaum, *Journal of Materials Science & Technology* 2019, vol. 35, pp. 368-376.
299) Y. Qin, P. Wen, M. Voshage, Y. Chen, P.G. Schückler, L. Jauer, D. Xia, H. Guo, Y. Zheng and J.H. Schleifenbaum, *Materials & Design* 2019, vol. 181, p. 107937.
300) Y. Li, P. Pavanram, J. Zhou, K. Lietaert, P. Taheri, W. Li, H. San, M.A. Leeflang, J.M.C. Mol, H. Jahr and A.A. Zadpoor, *Acta Biomaterialia* 2019, vol. 101, pp. 609-623.
301) A.H.M. Yusop, N.M. Daud, H. Nur, M.R.A. Kadir and H. Hermawan, *Scientific Reports* 2015, vol. 5, p. 11194.
302) R. Alavi, A. Trenggono, S. Champagne and H. Hermawan, *Metals* 2017, vol. 7.
303) H. Fayazfar, M. Salarian, A. Rogalsky, D. Sarker, P. Russo, V. Paserin and E. Toyserkani, *Materials & Design* 2018, vol. 144, pp. 98-128.
304) B. Song, S. Dong, S. Deng, H. Liao and C. Coddet, *Optics & Laser Technology* 2014, vol. 56, pp. 451-460.
305) B. Song, S. Dong, Q. Liu, H. Liao and C. Coddet, *Materials & Design (1980-2015)* 2014, vol. 54, pp. 727-733.

306) B. Zhang and C. Coddet, *Journal of Manufacturing Science and Engineering* 2015, vol. 138, pp. 051001-051001-9.

307) D. Palousek, L. Pantelejev, T. Zikmund and D. Koutny, *Modern Machinery Science Journal* 2017.

308) A. Simchi and H. Pohl, *Materials Science and Engineering: A* 2003, vol. 359, pp. 119-128.

309) L.-E. Loh, C.-K. Chua, W.-Y. Yeong, J. Song, M. Mapar, S.-L. Sing, Z.-H. Liu and D.-Q. Zhang, *International Journal of Heat and Mass Transfer* 2015, vol. 80, pp. 288-300.

310) M. Letenneur, V. Brailovski, A. Kreitcberg, V. Paserin and I. Bailon-Poujol, *Journal of Manufacturing and Materials Processing* 2017, vol. 1, p. 23.

311) D. Carluccio, M. Bermingham, D. Kent, A.G. Demir, B. Previtali and M.S. Dargusch, *Advanced Engineering Materials* 2019, vol. 0.

312) T. Niendorf, F. Brenne, P. Hoyer, D. Schwarze, M. Schaper, R. Grothe, M. Wiesener, G. Grundmeier and H.J. Maier, *Metallurgical and Materials Transactions A* 2015, vol. 46, pp. 2829-2833.

313) M. Wiesener, K. Peters, A. Taube, A. Keller, K.P. Hoyer, T. Niendorf and G. Grundmeier, *Materials and Corrosion* 2017, vol. 68, pp. 1028-1036.

314) D. Carluccio, A.G. Demir, L. Caprio, B. Previtali, M.J. Bermingham and M.S. Dargusch, *International Journal of Modern Physics B* 2019, vol. 34, p. 2040034.

315) D. Carluccio, A.G. Demir, L. Caprio, B. Previtali, M.J. Bermingham and M.S. Dargusch, *Journal of Manufacturing Processes* 2019, vol. 40, pp. 113-121.

316) Y. Li, H. Jahr, K. Lietaert, P. Pavanram, A. Yilmaz, L.I. Fockaert, M.A. Leeflang, B. Pouran, Y. Gonzalez-Garcia, H. Weinans, J.M.C. Mol, J. Zhou and A.A. Zadpoor, *Acta Biomaterialia* 2018, vol. 77, pp. 380-393.

317) D. Carluccio, C. Xu, J. Venezuela, Y. Cao, D. Kent, M. Bermingham, A.G. Demir, B. Previtali, Q. Ye and M. Dargusch, *Acta Biomaterialia* 2020, vol. 103, pp. 346-360.

318) T. Yamamoto, K. Fushimi, S. Miura and H. Konno, *Journal of The Electrochemical Society* 2010, vol. 157, pp. C231-C237.

319) Y. Li, K. Lietaert, W. Li, X.Y. Zhang, M.A. Leeflang, J. Zhou and A.A. Zadpoor, *Corrosion Science* 2019, vol. 156, pp. 106-116.

320) Y. Li, H. Jahr, P. Pavanram, F.S.L. Bobbert, U. Puggi, X.Y. Zhang, B. Pouran, M.A. Leeflang, H. Weinans, J. Zhou and A.A. Zadpoor, *Acta Biomaterialia* 2019, vol. 96, pp. 646-661.

321) Y. Li, P. Pavanram, J. Zhou, K. Lietaert, P. Taheri, W. Li, H. San, M.A. Leeflang, J.M.C. Mol, H. Jahr and A.A. Zadpoor, *Acta Biomaterialia* 2019.

322) J. Chen, P. Wu, Q. Wang, Y. Yang, S. Peng, Y. Zhou, C. Shuai and Y. Deng, *Metals* 2016, vol. 6, p. 259.

323) F. Witte, L. Jauer, W. Meiners, Z. Kronbach, K. Strohschein and T. Schmidt, In *10th World Biomaterials Congress*, (Frontiers Bionengineers and Biotechnology: Montreal, Canada, 2016).

324) T. DebRoy, H.L. Wei, J.S. Zuback, T. Mukherjee, J.W. Elmer, J.O. Milewski, A.M. Beese, A. Wilson-Heid, A. De and W. Zhang, *Progress in Materials Science* 2018, vol. 92, pp. 112-224.

325) L. Thijs, F. Verhaeghe, T. Craeghs, J.V. Humbeeck and J.-P. Kruth, *Acta Materialia* 2010, vol. 58, pp. 3303-3312.

326) P. Laakso, T. Riipinen, A. Laukkanen, T. Andersson, A. Jokinen, A. Revuelta and K. Ruusuvuori, *Physics Procedia* 2016, vol. 83, pp. 26-35.

327) A. Pawlak, M. Rosienkiewicz and E. Chlebus, *Archives of Civil and Mechanical Engineering* 2017, vol. 17, pp. 9-18.

328) N.A. Zumdick, L. Jauer, L.C. Kersting, T.N. Kutz, J.H. Schleifenbaum and D. Zander, *Materials Characterization* 2019, vol. 147, pp. 384-397.

329) S. Gangireddy, B. Gwalani, K. Liu, E.J. Faierson and R.S. Mishra, *Additive Manufacturing* 2019, vol. 26, pp. 53-64.

330) K. Lietaert, W. Baekelant, L. Thijs and J. Vleugels, In *European Congress and Exhibition on Powder Metallurgy. European PM Conference Proceedings*, (The European Powder Metallurgy Association: 2016), pp 1-6.

331) M. Grasso, A.G. Demir, B. Previtali and B.M. Colosimo, *Robotics and Computer-Integrated Manufacturing* 2018, vol. 49, pp. 229-239.
332) G. Catalano, A.G. Demir, V. Furlan and B. Previtali, *Journal of Micromechanics and Microengineering* 2018, vol. 28, p. 095016.
333) R. Yarovaya, I. Shklyarevskii and A. El-Shazly, *Soviet Journal of Experimental and Theoretical Physics* 1974, vol. 38, p. 331.
334) D. Schuöcker: *Handbook of the Eurolaser Academy*. (Springer Science & Business Media, 1998).
335) H.-J. Hagemann, W. Gudat and C. Kunz, *JOSA* 1975, vol. 65, pp. 742-744.
336) L. Loh, Z. Liu, D. Zhang, M. Mapar, S. Sing, C. Chua and W. Yeong, *Virtual and Physical Prototyping* 2014, vol. 9, pp. 11-16.
337) A. Okunkova, M. Volosova, P. Peretyagin, Y. Vladimirov, I. Zhirnov and A. Gusarov, *Physics Procedia* 2014, vol. 56, pp. 48-57.
338) M. Cloots, P.J. Uggowitzer and K. Wegener, *Materials & Design* 2016, vol. 89, pp. 770-784.
339) A.G. Demir, P. Colombo and B. Previtali, *The International Journal of Advanced Manufacturing Technology* 2017, vol. 91, pp. 2701-2714.
340) L. Caprio, A.G. Demir and B. Previtali, *Journal of Laser Applications* 2018, vol. 30, p. 032305.
341) A.G. Demir, L. Mazzoleni, L. Caprio, M. Pacher and B. Previtali, *Optics & Laser Technology* 2019, vol. 113, pp. 15-26.
342) L. Caprio, A.G. Demir and B. Previtali, *Journal of Materials Processing Technology* 2019, vol. 266, pp. 429-441.
343) C.A. Biffi, J. Fiocchi, P. Bassani and A. Tuissi, *Additive Manufacturing* 2018, vol. 24, pp. 639-646.
344) S. Catchpole-Smith, N. Aboulkhair, L. Parry, C. Tuck, I. Ashcroft and A. Clare, *Additive Manufacturing* 2017, vol. 15, pp. 113-122.
345) Y. Lu, S. Wu, Y. Gan, T. Huang, C. Yang, L. Junjie and J. Lin, *Optics & Laser Technology* 2015, vol. 75, pp. 197-206.
346) V. Finazzia, A.G. Demira, C.A. Biffic, C. Chiastrad, F. Migliavaccae, L. Petrinib and B. Previtalia, *Procedia Structural Integrity* 2019, vol. 15, pp. 16-23.
347) R. Stamp, P. Fox, W. O'neill, E. Jones and C. Sutcliffe, *Journal of Materials Science: Materials in Medicine* 2009, vol. 20, p. 1839.
348) E. Onal, A.E. Medvedev, M.A. Leeflang, A. Molotnikov and A.A. Zadpoor, *Additive Manufacturing* 2019, vol. 29, p. 100785.
349) M. Grasso and B.M. Colosimo, *Measurement Science and Technology* 2017, vol. 28, p. 044005.
350) M. Grasso, A. Demir, B. Previtali and B. Colosimo, *Robotics and Computer-Integrated Manufacturing* 2018, vol. 49, pp. 229-239.
351) L. Yuan, S. Ding and C. Wen, *Bioactive Materials* 2019, vol. 4, pp. 56-70.
352) X.P. Tan, Y.J. Tan, C.S.L. Chow, S.B. Tor and W.Y. Yeong, *Materials Science and Engineering: C* 2017, vol. 76, pp. 1328-1343.
353) F.S.L. Bobbert, K. Lietaert, A.A. Eftekhari, B. Pouran, S.M. Ahmadi, H. Weinans and A.A. Zadpoor, *Acta Biomaterialia* 2017, vol. 53, pp. 572-584.
354) N. Soro, H. Attar, E. Brodie, M. Veidt, A. Molotnikov and M.S. Dargusch, *Journal of the Mechanical Behavior of Biomedical Materials* 2019, vol. 97, pp. 149-158.
355) A.A. Zadpoor, *Journal of Materials Chemistry B* 2019, vol. 7, pp. 4088-4117.
356) X. Wang, S. Xu, S. Zhou, W. Xu, M. Leary, P. Choong, M. Qian, M. Brandt and Y.M. Xie, *Biomaterials* 2016, vol. 83, pp. 127-141.
357) F. Bobbert, K. Lietaert, A.A. Eftekhari, B. Pouran, S. Ahmadi, H. Weinans and A. Zadpoor, *Acta biomaterialia* 2017, vol. 53, pp. 572-584.
358) J. Shin, S. Kim, D. Jeong, H.G. Lee, D. Lee, J.Y. Lim and J. Kim, *Mathematical Problems in Engineering* 2012, vol. 2012, p. 13.

359) A.A. Zadpoor, *Biomaterials Science* 2015, vol. 3, pp. 231-245.
360) C.M. Bidan, K.P. Kommareddy, M. Rumpler, P. Kollmannsberger, P. Fratzl and J.W.C. Dunlop, *Advanced Healthcare Materials* 2013, vol. 2, pp. 186-194.
361) Y. Li, H. Jahr, P. Pavanram, F.S.L. Bobbert, U. Puggi, X.Y. Zhang, B. Pouran, M.A. Leeflang, H. Weinans, J. Zhou and A.A. Zadpoor, *Acta Biomaterialia* 2019.
362) A. Gökhan Demir and B. Previtali, *Biointerphases* 2014, vol. 9, p. 029004.
363) A. Thompson, I. Maskery and R.K. Leach, *Measurement Science and Technology* 2016, vol. 27, p. 072001.
364) G. Moroni and S. Petrò, *CIRP Annals* 2018, vol. 67, pp. 519-522.